

Integrable Lattice Realizations of Conformal Twisted Boundary Conditions

C.H. Otto Chui¹, Christian Mercat²
and Paul A. Pearce³

*Department of Mathematics and Statistics, University of Melbourne
Parkville, Victoria 3010, Australia*

Abstract

We study integrable realizations of conformal twisted boundary conditions for $sl(2)$ unitary minimal models on a torus. These conformal field theories are realized as the continuum scaling limit of critical $G = A, D, E$ lattice models with positive spectral parameter $u > 0$ and Coxeter number g . Integrable seams are constructed by fusing blocks of elementary local face weights. The usual A -type fusions are labelled by the Kac labels (r, s) and are associated with the Verlinde fusion algebra. We introduce a new type of fusion in the two braid limits $u \rightarrow \pm i\infty$ associated with the graph fusion algebra, and labelled by nodes $a, b \in G$ respectively. When combined with automorphisms, they lead to general integrable seams labelled by $x = (r, a, b, \kappa) \in (A_{g-2}, H, H, \mathbb{Z}_2)$ where H is the graph G itself for Type I theories and its parent for Type II theories. Identifying our construction labels with the conformal labels of Petkova and Zuber, we find that the integrable seams are in one-to-one correspondence with the conformal seams. The distinct seams are thus associated with the nodes of the Ocneanu quantum graph. The quantum symmetries and twisted partition functions are checked numerically for $|G| \leq 6$. We also show, in the case of $D_{2\ell}$, that the non-commutativity of the Ocneanu algebra of seams arises because the automorphisms do not commute with the fusions.

1 Introduction

There has been much recent progress [1, 2, 3, 4, 5, 6, 7, 8], on understanding integrable boundaries in statistical mechanics, conformal boundary conditions in rational conformal field theories and the intimate relations between them on both the cylinder and the torus. Indeed it appears that, for certain classes of theories, all of the conformal boundary conditions on a cylinder can be realized as the continuum scaling limit of integrable boundary conditions for the associated integrable lattice models. For $sl(2)$ minimal theories, a complete classification has been given [1, 2, 3] of the conformal boundary conditions on a cylinder.

¹Email: C.Chui@ms.unimelb.edu.au

²Present Address: Technische Universität, Berlin Sfb 288, Strasse des 17. Juni, 136, D-10623 Berlin, Germany; Email: Mercat@Sfb288.Math.TU-Berlin.de

³Email: P.Pearce@ms.unimelb.edu.au

These are labelled by nodes (r, a) of a tensor product graph $A \otimes G$ where the pair of graphs (A, G) , with G of A - D - E type, coincide precisely with the pairs in the A - D - E classification of Cappelli, Itzykson and Zuber [9]. Moreover, the physical content of the boundary conditions on the cylinder has been ascertained [4, 10] by studying the related integrable boundary conditions of the associated A - D - E lattice models [11] for both positive and negative spectral parameters, corresponding to *unitary minimal theories* and *parafermionic theories* respectively. Recently, the lattice realization of integrable and conformal boundary conditions for $N = 1$ *superconformal theories*, which correspond to the *fused A* lattice models with positive spectral parameter, has also been understood [12].

In this article, we use fusion to complete the task [13] of constructing integrable realizations of conformal twisted boundary conditions on the torus. Although the methods are very general we consider $sl(2)$ unitary minimal models for concreteness. The key idea is that fused blocks of elementary face weights on the lattice play the role of the local operators in the theory. The integrable and conformal boundary conditions on the cylinder are constructed [4] by acting with these fused blocks on the simple integrable boundary condition representing the vacuum. For the usual A -type fusion, associated with the Verlinde fusion algebra, this leads to integrable seams labelled by the Kac labels $(r, s) \in (A_{g-2}, A_{g-1})$. In this paper we introduce a new type of fusion of G -type related to the graph fusion algebra. Integrable seams of this type are labelled by $(r, a) \in (A_{g-2}, H)$ where H is the graph G itself for Type I theories and its parent for Type II theories. By the generalized Yang-Baxter equations, these fused blocks or seams can be propagated into the bulk without changing the spectrum of the theory. The seams so constructed provide integrable and conformal boundary conditions on the torus. Fixed boundary conditions $a \in G$ on the edge of the cylinder are propagated into the bulk by the action of the seam $(1, a)$ on the distinguished (vacuum) node $1 \in G$. Lastly, automorphism seams, which play no role on the cylinder, play a crucial role on the torus by providing the extra label giving rise to the complement of the left and right chiral subalgebras in the Ocneanu graph.

In general, for rational conformal field theories on the torus, we expect the two types of fusions supplemented by the automorphisms to generate all of the integrable and conformal seams. In this paper we discuss this assertion in the context of the A - D - E unitary minimal models.

The paper is organized as follows. In Section 2 we define the A - D - E series, giving their graphs (Sec. 2.1), their (proper or improper) graph fusion algebras (Sec. 2.2), their Ocneanu graphs (Sec. 2.3) and their associated twisted partition functions (Sec. 2.3 and 2.4). The presentation is self contained. In Section 3 we describe the lattice realization of these twisted boundary conditions. In particular, we define the A - D - E lattice models (Sec. 3.1), the fusion projectors (Sec. 3.2), the associated fused faces (Sec. 3.3) and the integrable seams (Sec. 3.4 to 3.6). We construct the transfer matrices in Section 4 composed of regular faces and seams. This is described for the single-row transfer matrix on the torus (Sec. 4.1) and the double-row transfer matrix on the cylinder (Sec. 4.3). The spectra of the transfer matrices and finite-size corrections are described in Section 5. The free energies are computed (Sec. 5.2) and the numerical conformal parts are identified with the twisted partition functions (Sec. 5.3 to

5.6).

2 A-D-E Fusion Graphs and Partition Functions

A-D-E classifications appear in a variety of contexts, namely, graphs, solvable lattice models, $\widehat{\mathfrak{sl}}(2)_k$ (Wess-Zumino-Witten) models at level k , and $sl(2)$ minimal models.

2.1 A-D-E Graphs

The basic *A-D-E* objects are graphs. A simple *graph* G is given by its *vertices* (or nodes) $a \in G_0$ and *edges* $(a, b) \in G_1 \subset G_0 \times G_0$. We are concerned with unoriented graphs, $(a, b) \in G_1 \Rightarrow (b, a) \in G_1$. The *A-D-E* graphs, which are the Dynkin diagrams of simply laced Lie algebras, are presented in Table 1. The number g is the Coxeter number of the graph G and the exponents $\text{Exp}(G)$ are a subset (with multiplicities) of the nodes of the A_L graph sharing the same Coxeter number as G .

	Graph G	g	$\text{Exp}(G)$	Type/H	Γ
A_L		$L + 1$	$1, 2, \dots, L$	I	\mathbb{Z}_2
$D_{\ell+2}$ (ℓ even)		$2\ell + 2$	$1, 3, \dots, 2\ell + 1, \ell + 1$	I	\mathbb{Z}_2
$D_{\ell+2}$ (ℓ odd)		$2\ell + 2$	$1, 3, \dots, 2\ell + 1, \ell + 1$	II/ $A_{2\ell+1}$	\mathbb{Z}_2
E_6		12	$1, 4, 5, 7, 8, 11$	I	\mathbb{Z}_2
E_7		18	$1, 5, 7, 9, 11, 13, 17$	II/ D_{10}	1
E_8		30	$1, 7, 11, 13, 17, 19, 23, 39$	I	1

Figure 1: *A-D-E* graphs corresponding to the Dynkin diagrams of the classical *A-D-E* simply laced Lie algebras. The nodes associated with the identity and the fundamental are shown by $*$, \square respectively. Also shown are the Coxeter numbers g , exponents $\text{Exp}(G)$, the Type I or II, the parent graphs $H \neq G$ and the diagram automorphism group Γ . The D_4 graph is exceptional having the automorphism group \mathbb{S}_3 .

A graph G is completely encoded by its adjacency matrix which we denote by the same letter G . It is a symmetric non-negative integer square matrix whose rows and columns are labelled by the vertices of G , defined by $G_{ab} = 1$ if a and b are adjacent and $G_{ab} = 0$

otherwise. What is so special about the A - D - E graphs is that (along with the tadpole⁴ series) they are the only ones whose spectra lies in the open interval $(-2, 2)$. The Perron-Frobenius theorem implies that the largest eigenvalue of these adjacency matrices is non-degenerate, real and positive and its eigenvector can be chosen to have non-negative entries. They are given explicitly in terms of q -deformed integers $S_n = [n]_q = \frac{q^n - q^{-n}}{q - q^{-1}}$ with $q = \exp(\pi i/g)$. The largest eigenvalue is $S_2 = [2]_q$ and the eigenvector ψ is

$$\begin{aligned}\psi_{A_L} &= ([k]_q),_{1 \leq k \leq L} \\ \psi_{D_{\ell+2}} &= ([k]_q,_{1 \leq k \leq \ell}, \frac{[\ell]_q}{[2]_q}, \frac{[\ell]_q}{[2]_q}) \\ \psi_{E_6} &= ([1]_q, [2]_q, [3]_q, [2]_q, [1]_q, \frac{[3]_q}{[2]_q}) \\ \psi_{E_7} &= ([1]_q, [2]_q, [3]_q, [4]_q, \frac{[6]_q}{[2]_q}, \frac{[4]_q}{[3]_q}, \frac{[4]_q}{[2]_q}) \\ \psi_{E_8} &= ([1]_q, [2]_q, [3]_q, [4]_q, [5]_q, \frac{[7]_q}{[2]_q}, \frac{[5]_q}{[3]_q}, \frac{[5]_q}{[2]_q}).\end{aligned}\tag{2.1}$$

2.2 Graph fusion algebras

The integer linear span of the nodes of the graph can be given a structure of a commutative *graph fusion algebra*. We first specify two vertices, the identity vertex $*$ and the fundamental vertex \square . They are indicated in Table 1 and are respectively the vertices labelled 1 and 2 in the A_L , $D_{2\ell+2}$, E_6 and E_8 cases, known as Type I theories, the vertices $2\ell+1$ and $2\ell-1$ for the $D_{2\ell+1}$ case, and the vertices 1, 2 for the E_7 case, known as Type II theories. The former models give rise to proper graph fusion algebras with non negative integer structure constants or Non-negative Integer Matrix Irreducible Representations (nimreps) which are understood as adjacency matrices. The latter have some negative structure constants and do not form proper graph fusion algebras.

The algebra is defined by stating that the edges of the graph G encode the action of the fundamental element \square :

$$a \square = \sum_{b \sim a} b.\tag{2.2}$$

The identity gives one row of the algebra table, the previous formula gives another, commutativity and associativity determine the rest. On the D_4 example, $\square = 2$ and associativity gives

$$\begin{aligned}(4 - 3)(\square \square) &= (4 \square - 3 \square) \square = 0 \\ &= (4 - 3)(1 + 3 + 4)\end{aligned}\tag{2.3}$$

so that $4 - 3 = 3 \ 3 - 4 \ 4$ and $\square \ 3 \ 3 = \square$ shows that $\begin{cases} 3 \ 3 = 4 \\ 4 \ 4 = 3 \end{cases}$ and the expansion of $3 \ 3 \ 3$ implies $3 \ 4 = 1$.

⁴The tadpole graph T_L is obtained from the graph A_L by adding a loop at the final vertex; it is not a simple graph.

The structure constants of this algebra are denoted \hat{N}

$$ab = \sum_{c \in G} \hat{N}_{a b}^c c. \quad (2.4)$$

The definition of the algebra implies $\hat{N}_* = I$ and $\hat{N}_\square = G$ and these matrices themselves form the regular representation of the algebra with the usual matrix product

$$\hat{N}_a \hat{N}_b = \sum_{c \in G} \hat{N}_{a b}^c \hat{N}_c. \quad (2.5)$$

As it is a commutative algebra containing the adjacency matrix, its common set of eigenvectors is given by an orthogonal basis of eigenvectors of G . They are labelled by Coxeter exponents (we have only given the Perron-Frobenius eigenvector) and the spectral decomposition of each matrix onto its eigenvectors give these integers through a Verlinde-like formula

$$\hat{N}_{a b}^c = \sum_{j \in \text{Exp}(G)} \frac{\psi_a^j \psi_b^j (\psi_c^j)^*}{\psi_*^j}. \quad (2.6)$$

Some algebra tables are given in Tables 1–5. In the case of the graph A_L this reduces to the usual Verlinde formula, the structure constants are denoted by $N_{i j}^k$ and the matrix of eigenvectors by S . For an A - D - E graph G with Coxeter number $g = L + 1$, another algebra of non-negative integer matrices with the A_L structure constants $N_{i j}^k$ is given by the *fused adjacency matrices* n_i defined by the $sl(2)$ recurrence relation

$$n_1 = I, \quad n_2 = G, \quad n_{i+1} = n_2 n_i - n_{i-1} \quad \text{for } 2 < i < g - 1, \quad (2.7)$$

which closes with $n_i = 0$ for $i > g - 2$ and

$$n_{g-2} = \begin{cases} I, & \text{for } D_{2\ell}, E_7, E_8 \\ \sigma, & \text{for } A_L, D_{2\ell-1}, E_6 \end{cases} \quad (2.8)$$

where σ is the \mathbf{Z}_2 graph automorphism. Clearly, E_7 and E_8 do not admit a \mathbf{Z}_2 automorphism. So the fusions contain the \mathbf{Z}_2 graph automorphism in all cases where it exists except for $D_{2\ell}$.

The matrices n_i also satisfy a Verlinde like property

$$n_{i a}^b = \sum_{j \in \text{Exp}(G)} \frac{S_i^j}{S_*^j} \psi_a^j (\psi_b^j)^* \quad (2.9)$$

with the algebra structure

$$n_i n_j = \sum_{k \in A_L} N_{i j}^k n_k, \quad n_i \hat{N}_a = \sum_{b \in G} n_{i a}^b \hat{N}_b. \quad (2.10)$$

The matrices n_i are in fact linear combinations of the graph algebra matrices \hat{N}_a

$$n_i = \sum_{a \in G} n_{i 1}^a \hat{N}_a. \quad (2.11)$$

$$N_1 = \begin{pmatrix} 1 & 0 & 0 & 0 \\ 0 & 1 & 0 & 0 \\ 0 & 0 & 1 & 0 \\ 0 & 0 & 0 & 1 \end{pmatrix}, \quad N_2 = \begin{pmatrix} 0 & 1 & 0 & 0 \\ 1 & 0 & 1 & 0 \\ 0 & 1 & 0 & 1 \\ 0 & 0 & 1 & 0 \end{pmatrix}, \quad N_3 = \begin{pmatrix} 0 & 0 & 1 & 0 \\ 0 & 1 & 0 & 1 \\ 1 & 0 & 1 & 0 \\ 0 & 1 & 0 & 0 \end{pmatrix}, \quad N_4 = \begin{pmatrix} 0 & 0 & 0 & 1 \\ 0 & 0 & 1 & 0 \\ 0 & 1 & 0 & 0 \\ 1 & 0 & 0 & 0 \end{pmatrix}.$$

	1	2	3	4	
1	1	2	3	4	$Z_1 = \chi_1\chi_1^* + \chi_2\chi_2^* + \chi_3\chi_3^* + \chi_4\chi_4^*$
2	2	1+3	2+4	3	$Z_2 = \chi_2\chi_1^* + (\chi_1 + \chi_3)\chi_2^* + (\chi_2 + \chi_4)\chi_3^* + \chi_3\chi_4^*$
3	3	2+4	1+3	2	$Z_3 = \chi_3\chi_1^* + (\chi_2 + \chi_4)\chi_2^* + (\chi_1 + \chi_3)\chi_3^* + \chi_2\chi_4^*$
4	4	3	2	1	$Z_4 = \chi_4\chi_1^* + \chi_3\chi_2^* + \chi_2\chi_3^* + \chi_1\chi_4^*$

Table 1: Fusion matrices, graph fusion algebra and twisted partition functions of A_4 in terms of affine $sl(2)$ characters χ_s .

$$\hat{N}_1 = \begin{pmatrix} 1 & 0 & 0 & 0 \\ 0 & 1 & 0 & 0 \\ 0 & 0 & 1 & 0 \\ 0 & 0 & 0 & 1 \end{pmatrix}, \quad \hat{N}_2 = \begin{pmatrix} 0 & 1 & 0 & 0 \\ 1 & 0 & 1 & 1 \\ 0 & 1 & 0 & 0 \\ 0 & 1 & 0 & 0 \end{pmatrix}, \quad \hat{N}_3 = \begin{pmatrix} 0 & 0 & 1 & 0 \\ 0 & 1 & 0 & 0 \\ 0 & 0 & 0 & 1 \\ 1 & 0 & 0 & 0 \end{pmatrix}, \quad \hat{N}_4 = \begin{pmatrix} 0 & 0 & 0 & 1 \\ 0 & 1 & 0 & 0 \\ 1 & 0 & 0 & 0 \\ 0 & 0 & 1 & 0 \end{pmatrix}.$$

	1	2	3	4	
1	1	2	3	4	$Z_1 = \hat{\chi}_1\hat{\chi}_1^* + \hat{\chi}_3\hat{\chi}_3^* + \hat{\chi}_4\hat{\chi}_4^*$
2	2	1+3+4	2	2	$Z_{2\otimes 1} = \hat{\chi}_2\hat{\chi}_1^* + \hat{\chi}_2\hat{\chi}_3^* + \hat{\chi}_2\hat{\chi}_4^* = Z_{1\otimes 2}^*$
3	3	2	4	1	$Z_3 = \hat{\chi}_3\hat{\chi}_1^* + \hat{\chi}_4\hat{\chi}_3^* + \hat{\chi}_1\hat{\chi}_4^* = Z_4$
4	4	2	1	3	$Z_4 = \hat{\chi}_4\hat{\chi}_1^* + \hat{\chi}_1\hat{\chi}_3^* + \hat{\chi}_3\hat{\chi}_4^*$
					$Z_{1'} = Z_{3'} = Z_{4'} = \hat{\chi}_2\hat{\chi}_2^*$

$$\hat{\chi}_1 = \chi_1 + \chi_5, \quad \hat{\chi}_2 = \chi_2 + \chi_4, \quad \hat{\chi}_3 = \hat{\chi}_4 = \chi_3$$

	1	2	3	4	1'	2'	3'	4'	
1	1	2	3	4	1'	2'	3'	4'	
2	2	1+3+4	2	2	2'	1'+3'+4'	2'	2'	
3	3	2	4	1	3'	2'	4'	1'	
4	4	2	1	3	4'	2'	1'	3'	
1'	1'	2'	4'	3'	1	2	4	3	
2'	2'	1'+3'+4'	2'	2'	2	1+3+4	2	2	
3'	3'	2'	1'	4'	3	2	1	4	
4'	4'	2'	3'	1'	4	2	3	1	

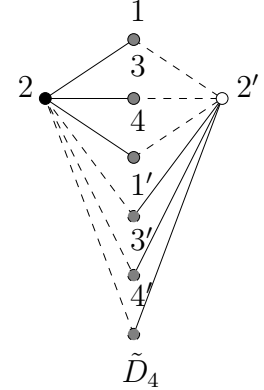


Table 2: Fusion matrices, graph fusion algebra, twisted partition functions, Ocneanu algebra and Ocneanu graph of D_4 . The extended chiral and ambichiral subalgebras are bold.

$$\hat{N}_1 = \begin{pmatrix} 0 & -1 & 0 & 1 & 1 \\ -1 & 0 & 1 & 0 & 0 \\ 0 & 1 & 0 & 0 & 0 \\ 1 & 0 & 0 & 0 & 0 \\ 1 & 0 & 0 & 0 & 0 \end{pmatrix}, \quad \hat{N}_2 = \begin{pmatrix} -1 & 0 & 1 & 0 & 0 \\ 0 & 0 & 0 & 1 & 1 \\ 1 & 0 & 1 & 0 & 0 \\ 0 & 1 & 0 & 0 & 0 \\ 0 & 0 & 1 & 0 & 0 \end{pmatrix}, \quad \hat{N}_3 = \begin{pmatrix} 0 & 1 & 0 & 0 & 0 \\ 1 & 0 & 1 & 0 & 0 \\ 0 & 1 & 0 & 1 & 1 \\ 0 & 0 & 1 & 0 & 1 \\ 0 & 0 & 1 & 1 & 0 \end{pmatrix},$$

$$\hat{N}_4 = \begin{pmatrix} 1 & 0 & 0 & 0 & 0 \\ 0 & 1 & 0 & 0 & 0 \\ 0 & 0 & 1 & 0 & 0 \\ 0 & 0 & 0 & 1 & 0 \\ 0 & 0 & 0 & 0 & 1 \end{pmatrix}, \quad \hat{N}_5 = \begin{pmatrix} 1 & 0 & 0 & 0 & 0 \\ 0 & 1 & 0 & 0 & 0 \\ 0 & 0 & 1 & 0 & 0 \\ 0 & 0 & 0 & 1 & 0 \\ 0 & 0 & 0 & 0 & 1 \end{pmatrix}.$$

Table 3: The D_5 graph fusion algebra is not a proper graph algebra.

$$\hat{N}_1 = \begin{pmatrix} 1 & 0 & 0 & 0 & 0 & 0 \\ 0 & 1 & 0 & 0 & 0 & 0 \\ 0 & 0 & 1 & 0 & 0 & 0 \\ 0 & 0 & 0 & 1 & 0 & 0 \\ 0 & 0 & 0 & 0 & 1 & 0 \\ 0 & 0 & 0 & 0 & 0 & 1 \end{pmatrix}, \quad \hat{N}_2 = \begin{pmatrix} 0 & 1 & 0 & 0 & 0 & 0 \\ 1 & 0 & 1 & 0 & 0 & 0 \\ 0 & 1 & 0 & 1 & 0 & 0 \\ 0 & 0 & 1 & 0 & 1 & 1 \\ 0 & 0 & 0 & 1 & 0 & 0 \\ 0 & 0 & 0 & 1 & 0 & 0 \end{pmatrix}, \quad \hat{N}_3 = \begin{pmatrix} 0 & 0 & 1 & 0 & 0 & 0 \\ 0 & 1 & 0 & 1 & 0 & 0 \\ 1 & 0 & 1 & 0 & 1 & 1 \\ 0 & 1 & 0 & 2 & 0 & 0 \\ 0 & 0 & 1 & 0 & 0 & 1 \\ 0 & 0 & 1 & 0 & 1 & 0 \end{pmatrix},$$

$$\hat{N}_4 = \begin{pmatrix} 0 & 0 & 0 & 1 & 0 & 0 \\ 0 & 0 & 0 & 0 & 1 & 1 \\ 0 & 1 & 0 & 2 & 0 & 0 \\ 1 & 0 & 2 & 0 & 1 & 1 \\ 0 & 1 & 0 & 1 & 0 & 0 \\ 0 & 1 & 0 & 1 & 0 & 0 \end{pmatrix}, \quad \hat{N}_5 = \begin{pmatrix} 0 & 0 & 0 & 0 & 1 & 0 \\ 0 & 0 & 0 & 1 & 0 & 0 \\ 0 & 0 & 1 & 0 & 0 & 1 \\ 0 & 1 & 0 & 1 & 0 & 0 \\ 1 & 0 & 0 & 0 & 1 & 0 \\ 0 & 0 & 1 & 0 & 0 & 0 \end{pmatrix}, \quad \hat{N}_6 = \begin{pmatrix} 0 & 0 & 0 & 0 & 0 & 1 \\ 0 & 0 & 0 & 1 & 0 & 0 \\ 0 & 0 & 1 & 0 & 1 & 0 \\ 0 & 1 & 0 & 1 & 0 & 0 \\ 0 & 0 & 1 & 0 & 0 & 0 \\ 1 & 0 & 0 & 0 & 0 & 1 \end{pmatrix},$$

	1	2	3	4	5	6
1	1	2	3	4	5	6
2	2	1+3	2+4	3+5+6	4	4
3	3	2+4	1+ 3+5+6	2+4+4	3+6	3+5
4	4	3+5+6	1+3+3+5+6	2+4	2+4	
5	5	4	3+6	2+4	1+5	3
6	6	4	3+5	2+4	3	1+6

$$\begin{aligned}
Z_1 &= \hat{\chi}_1 \hat{\chi}_1^* + \hat{\chi}_3 \hat{\chi}_3^* + \hat{\chi}_5 \hat{\chi}_5^* + \hat{\chi}_6 \hat{\chi}_6^*, \\
Z_{2 \otimes 1} &= \hat{\chi}_2 \hat{\chi}_1^* + (\hat{\chi}_2 + \hat{\chi}_4) \hat{\chi}_3^* + \hat{\chi}_4 (\hat{\chi}_5 + \hat{\chi}_6)^* = Z_{1 \otimes 2}^*, \\
Z_3 &= \hat{\chi}_3 \hat{\chi}_1^* + (\hat{\chi}_1 + \hat{\chi}_3 + \hat{\chi}_5 + \hat{\chi}_6) \hat{\chi}_3^* + (\hat{\chi}_3 + \hat{\chi}_6) \hat{\chi}_5^* + (\hat{\chi}_3 + \hat{\chi}_5) \hat{\chi}_6^*, \\
Z_{4 \otimes 1} &= \hat{\chi}_4 \hat{\chi}_1^* + (\hat{\chi}_2 + 2\hat{\chi}_4) \hat{\chi}_3^* + (\hat{\chi}_2 + \hat{\chi}_4) (\hat{\chi}_5 + \hat{\chi}_6)^* = Z_{1 \otimes 4}^*, \\
Z_5 &= \hat{\chi}_5 \hat{\chi}_1^* + (\hat{\chi}_3 + \hat{\chi}_6) \hat{\chi}_3^* + (\hat{\chi}_1 + \hat{\chi}_5) \hat{\chi}_5^* + \hat{\chi}_3 \hat{\chi}_6^*, \\
Z_6 &= \hat{\chi}_6 \hat{\chi}_1^* + (\hat{\chi}_3 + \hat{\chi}_5) \hat{\chi}_3^* + \hat{\chi}_3 (\hat{\chi}_1 + \hat{\chi}_6) \hat{\chi}_5^* + (\hat{\chi}_1 + \hat{\chi}_6) \hat{\chi}_6^*, \\
Z_{1'} &= \hat{\chi}_2 \hat{\chi}_2^* + \hat{\chi}_4 \hat{\chi}_4^*, \\
Z_{3'} &= |\hat{\chi}_2 + \hat{\chi}_4|^2 + |\hat{\chi}_4|^2, \\
Z_{5'} &= Z_{6'} = \hat{\chi}_2 \hat{\chi}_4^* + \hat{\chi}_4 \hat{\chi}_2^* + |\hat{\chi}_4|^2.
\end{aligned}$$

$$\hat{\chi}_1 = \chi_1 + \chi_9, \quad \hat{\chi}_2 = \chi_2 + \chi_8, \quad \hat{\chi}_3 = \chi_3 + \chi_7,$$

$$\hat{\chi}_4 = \chi_4 + \chi_6, \quad \hat{\chi}_5 = \hat{\chi}_6 = \chi_5.$$

Table 4: The graph fusion algebra of D_6 and its twisted partition functions in terms of extended characters. The extended chiral subalgebra T is shown bold (see Fig. 4) and the extended characters are given in terms of the A_9 characters.

$$\begin{aligned}\hat{N}_1 &= \begin{pmatrix} 1 & 0 & 0 & 0 & 0 & 0 \\ 0 & 1 & 0 & 0 & 0 & 0 \\ 0 & 0 & 1 & 0 & 0 & 0 \\ 0 & 0 & 0 & 1 & 0 & 0 \\ 0 & 0 & 0 & 0 & 1 & 0 \\ 0 & 0 & 0 & 0 & 0 & 1 \end{pmatrix}, \quad \hat{N}_2 = \begin{pmatrix} 0 & 1 & 0 & 0 & 0 & 0 \\ 1 & 0 & 1 & 0 & 0 & 0 \\ 0 & 0 & 1 & 0 & 0 & 1 \\ 0 & 0 & 0 & 1 & 0 & 0 \\ 0 & 0 & 0 & 0 & 1 & 0 \\ 0 & 0 & 1 & 0 & 0 & 0 \end{pmatrix}, \quad \hat{N}_3 = \begin{pmatrix} 0 & 0 & 1 & 0 & 0 & 0 \\ 0 & 1 & 0 & 1 & 0 & 1 \\ 1 & 0 & 2 & 0 & 1 & 0 \\ 0 & 1 & 0 & 1 & 0 & 1 \\ 0 & 0 & 1 & 0 & 0 & 0 \\ 0 & 1 & 0 & 1 & 0 & 0 \end{pmatrix}, \\ \hat{N}_4 &= \begin{pmatrix} 0 & 0 & 0 & 1 & 0 & 0 \\ 0 & 0 & 1 & 0 & 1 & 0 \\ 0 & 1 & 0 & 1 & 0 & 1 \\ 1 & 0 & 1 & 0 & 0 & 0 \\ 0 & 1 & 0 & 0 & 0 & 0 \\ 0 & 0 & 1 & 0 & 0 & 0 \end{pmatrix}. \quad \hat{N}_5 = \begin{pmatrix} 0 & 0 & 0 & 0 & 1 & 0 \\ 0 & 0 & 0 & 1 & 0 & 0 \\ 0 & 0 & 1 & 0 & 0 & 0 \\ 0 & 1 & 0 & 0 & 0 & 0 \\ 1 & 0 & 0 & 0 & 0 & 0 \\ 0 & 0 & 0 & 0 & 0 & 1 \end{pmatrix}, \quad \hat{N}_6 = \begin{pmatrix} 0 & 0 & 0 & 0 & 0 & 1 \\ 0 & 0 & 1 & 0 & 0 & 0 \\ 0 & 1 & 0 & 1 & 0 & 0 \\ 0 & 0 & 1 & 0 & 0 & 0 \\ 0 & 0 & 0 & 0 & 0 & 1 \\ 1 & 0 & 0 & 0 & 1 & 0 \end{pmatrix}.\end{aligned}$$

	1	2	3	4	5	6
1	1	2	3	4	5	6
2	2	1+3	2+4+6	3+5	4	3
3	3	2+4+6	1+3+3+5	2+4+6	3	2+4
4	4	3+5	2+4+6	1+3	2	3
5	5	4	3	2	1	6
6	6	3	2+4	3	6	1+5

$$\begin{aligned}Z_1 &= \hat{\chi}_1 \hat{\chi}_1^* + \hat{\chi}_5 \hat{\chi}_5^* + \hat{\chi}_6 \hat{\chi}_6^*, \\ Z_{2 \otimes 1} &= \hat{\chi}_2 \hat{\chi}_1^* + \hat{\chi}_4 \hat{\chi}_5^* + \hat{\chi}_3 \hat{\chi}_6^* = Z_{1 \otimes 2}^*, \\ Z_{3 \otimes 1} &= \hat{\chi}_3 \hat{\chi}_1^* + \hat{\chi}_3 \hat{\chi}_5^* + (\hat{\chi}_2 + \hat{\chi}_4) \hat{\chi}_6^* = Z_{1 \otimes 3}^*, \\ Z_{4 \otimes 1} &= \hat{\chi}_4 \hat{\chi}_1^* + \hat{\chi}_2 \hat{\chi}_5^* + \hat{\chi}_3 \hat{\chi}_6^* = Z_{1 \otimes 4}^*, \\ Z_5 &= \hat{\chi}_5 \hat{\chi}_1^* + \hat{\chi}_1 \hat{\chi}_5^* + \hat{\chi}_6 \hat{\chi}_6^*, \\ Z_6 &= \hat{\chi}_6 \hat{\chi}_1^* + \hat{\chi}_6 \hat{\chi}_5^* + (\hat{\chi}_1 + \hat{\chi}_5) \hat{\chi}_6^*.\end{aligned}$$

$$\hat{\chi}_1 = \chi_1 + \chi_7, \quad \hat{\chi}_2 = \chi_2 + \chi_6 + \chi_8, \quad \hat{\chi}_3 = \chi_3 + \chi_5 + \chi_7 + \chi_9,$$

$$\hat{\chi}_4 = \chi_4 + \chi_6 + \chi_{10}, \quad \hat{\chi}_5 = \chi_5 + \chi_{11}, \quad \hat{\chi}_6 = \chi_4 + \chi_8.$$

Table 5: The graph fusion algebra of E_6 and its twisted partition functions in terms of extended characters. The ambichiral subalgebra is shown bold and the extended characters are given in terms of the A_{11} characters.

For $b \in G$, the rectangular matrix $V^b = (n_{i,a}^b)_{i \in A_{g-1}, a \in G}$ is called an *intertwiner* because it intertwines the fused adjacency matrices:

$$N_i V^b = V^b n_i, \quad \text{for all } i \in A_L. \quad (2.12)$$

One view of these graph algebras is that nodes label bimodules and edges are homomorphisms between these bimodules. In the case of the graph G , the edges describe the homomorphisms arising from tensoring with the fundamental bimodule, the result is isomorphic to the direct sum of the bimodules which are adjacent to it on the graph. For Type I models, one can associate a graph G_a to each vertex in the same manner, by placing $\hat{N}_{a,b}^c$ edges between the vertex b and the vertex c . For Type II models, this construction fails.

The graph fusion algebra of a solvable A - D - E lattice model built on the graph G is not the graph fusion algebra itself. Rather, this latter graph encodes the fusion algebra of a *Wess-Zumino-Witten* $\widehat{sl}(2)_{g-2}$ (WZW) theory. The solvable A - D - E lattice model is actually associated with a *minimal model* whose fusion algebra is given by the *tensor product graph* $A_{g-2} \times G$ where g is the Coxeter number of G . A vertex of this tensor product graph is of the form $(r, a) \in A_{g-2} \times G$ and is adjacent with the vertex (r', b) whenever r and r' are neighbours in A_{g-2} and a and b are neighbours in G . When $G = A_{g-1}$, it is customary to denote such a vertex with the Kac labels (r, s) . Moreover, this tensor product graph is quotiented by the Kac table symmetry

$$(r, s) \sim (g-1-r, g-s) \quad \text{if } G = A_{g-1}, \quad (2.13)$$

$$(r, a) \sim (g-1-r, a) \quad \text{otherwise.} \quad (2.14)$$

The graph fusion algebra for this quotient is $A_{g-2} \otimes G / \sim$ and hence it is generated by the two $\widehat{sl}(2)$ WZW subalgebras $1 \otimes G$ and $A_{g-2} \otimes 1$.

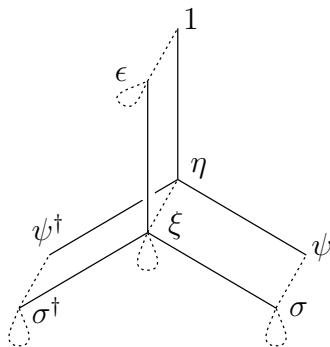


Figure 2: The graph (T_2, D_4) coding the fusion algebra of the three-state Potts model. The plain edges correspond to the multiplication by η , the dotted ones by ϵ . The nodes $(r, a) = \{(1, 1), (1, 2), (1, 3), (1, 4), (2, 1), (2, 2), (2, 3), (2, 4)\}$ in (T_2, D_4) are labelled by the associated fields $\{1, \eta, \psi, \psi^\dagger, \epsilon, \xi, \sigma, \sigma^\dagger\}$ respectively.

For example, the three-state Potts model is the minimal model associated with the graph D_4 . Its fusion algebra is the graph algebra $(A_4, D_4)/\sim = (T_2, D_4)$ pictured in Fig. 2.

It has eight vertices and two types of edges, corresponding to the action of the generators ϵ, η , of each subalgebra, $T_2 = \{I, \epsilon\}$ and $D_4 = \{I, \eta, \psi, \psi^\dagger\}$ where we use the labelling of Fig. 2. You read off that $\xi\eta = \epsilon + \sigma + \sigma^\dagger$ and $\xi\epsilon = \xi + \eta$. Assuming associativity, you can then infer for example that $\xi\xi = I + \epsilon + \psi + \psi^\dagger + \sigma + \sigma^\dagger$ and work out the rest of the algebra table, which is also given by the tensor product of the \hat{N} matrices for D_4 (listed in Table 2) with the fusion matrices of T_2 , namely

$$N_1 = \begin{pmatrix} 1 & 0 \\ 0 & 1 \end{pmatrix}, \quad N_2 = \begin{pmatrix} 0 & 1 \\ 1 & 1 \end{pmatrix}. \quad (2.15)$$

2.3 Ocneanu graph algebras and twisted partition functions

In this section we review the properties of Ocneanu (quantum double) graphs and their fusion algebras [7, 8, 14, 15, 16]. The related *Double Triangle Algebra* (DTA) governs many aspects of both the statistical mechanics models and their associated conformal field theories. It is called the algebra of *quantum symmetries* of the problem. We are interested here in the algebra of twisted boundary conditions on the torus, called the *twisted fusion algebra* [7, 8]. We discuss the twisted boundary conditions and associated twisted partition functions briefly summarizing the work of Petkova and Zuber [7, 8]. We then present an alternative approach using tensor products [14, 15, 16].

The twisted boundary conditions are encoded by the Ocneanu [14] graph fusion algebra \tilde{G} whose structure constants are denoted by \tilde{N}_{xy}^z for $x, y, z \in \tilde{G}$. The matrices $\tilde{N}_y = \{\tilde{N}_{xy}^z\}$ satisfy

$$\tilde{N}_x \tilde{N}_y = \sum_{z \in \tilde{G}} \tilde{N}_{xy}^z \tilde{N}_z. \quad (2.16)$$

Petkova and Zuber give explicit expressions for these structure constants for the *A-D-E* graphs. The seam index

$$x = \begin{cases} (a, b, \kappa) \in (H, H, \mathbf{Z}_2), & \text{WZW} \\ (r, a, b, \kappa) \in (A_{g-2}, H, H, \mathbf{Z}_2), & \text{minimal} \end{cases} \quad (2.17)$$

labels conformal twisted boundary conditions or seams. The index $\kappa = 1, 2$ labels the automorphisms $\eta = \sigma^{\kappa-1} = I, \sigma$. The seams x are not all distinct due to quantum symmetry

$$x = (r, a, b, \kappa) \equiv x' = (r', a', b', \kappa') \Leftrightarrow Z_{(r,a,b,\kappa)} = Z_{(r',a',b',\kappa')} \quad (2.18)$$

that is, seams giving rise to the same twisted partition functions are considered equivalent. In some cases, such as D_4 , it is necessary to use unspecialized characters to see the full quantum symmetry. For the WZW models, it suffices to take x of the form

$$x = \begin{cases} s \in A_{g-1}, & G = A_{g-1} \\ (a, \kappa) \in (D_{2\ell}, \mathbf{Z}_2), & G = D_{2\ell} \\ s \in A_{4\ell-1}, & G = D_{2\ell+1} \\ (a, b) \in (G, G), & G = E_{6,8} \\ (a, b) \in (D_{10}, D_{10}), & G = E_7 \end{cases} \quad (2.19)$$

and similarly for the minimal models with $r \in A_{g-2}$ added.

The modular invariant torus partition functions of the A - D - E minimal models are

$$Z(q) = \sum_{(r,s),(\bar{r},\bar{s})} Z_{(r,s),(\bar{r},\bar{s})} \chi_{r,s}(q) \chi_{\bar{r},\bar{s}}(\bar{q}), \quad Z_{(r,s),(\bar{r},\bar{s})} = \delta_{r,\bar{r}} \sum_{a \in T} n_{s1}^a n_{\bar{s}1}^{\zeta(a)} \quad (2.20)$$

where $n_s = n_s(H)$ are the fusion matrices of the Type I parent H of G ,

$$T = T_1 = \begin{cases} \{1, 2, \dots, L\}, & G = A_L \\ \{1, 3, 5, \dots, 2\ell - 1, 2\ell\}, & G = D_{2\ell} \\ \{1, 3, 5, \dots, 4\ell - 1\}, & G = D_{2\ell+1} \\ \{1, 5, 6\}, & G = E_6 \\ \{1, 3, 5, 7, 9, 10\}, & G = E_7 \\ \{1, 7\}, & G = E_8 \end{cases} \quad (2.21)$$

and the involutive twist ζ is the identity for Type I theories but for Type II theories has the action

$$\zeta = \begin{cases} s \mapsto 4\ell - s, s = 2, 4, \dots, 2\ell - 2, & G = D_{2\ell+1} \\ \{1, 3, 5, 7, 9, 10\} \mapsto \{1, 9, 5, 7, 3, 10\}, & G = E_7 \end{cases} \quad (2.22)$$

The twisted partition functions are given by the toric matrices $P_{ab}^{(\kappa)}$

$$Z_{(r,a,b,\kappa)}(q) = \sum_{(r,s),(\bar{r},\bar{s})} \delta_{r,\bar{r}} [P_{ab}^{(\kappa)}]_{s\bar{s}} \chi_{r,s}(q) \chi_{\bar{r},\bar{s}}(\bar{q}), \quad [P_{ab}^{(\kappa)}]_{s\bar{s}} = \sum_{c \in T_\kappa} n_{sa}^c n_{\bar{s}b}^{\zeta(c)} \quad (2.23)$$

where

$$T_2 = \begin{cases} \{2, 4, \dots, 2\ell - 2\}, & G = D_{2\ell} \\ T_1, & \text{otherwise} \end{cases} \quad (2.24)$$

except for the special seams denoted $x = (r, X)$ of E_7 [8], which are given by $Z_{(r,X)}(q) = Z_{(r,6,2,1)}(q) - Z_{(r,4,2,1)}(q)$.

The Ocneanu graph fusion algebra is a double graph algebra combining left and right copies of the graph fusion algebra H connected through a left-right symmetric subalgebra called the *ambichiral subalgebra*. For graphs G of Type I, H is G itself. For graphs G of Type II, it involves the parent graph algebra H and a twist ζ . Although the graph algebras of Type II theories are not proper graph algebras, the parent graph H is always of Type I. The Ocneanu graph has two types of edges (plain and dashed), corresponding to the action of the left and right copies of the generator of H .

An alternative construction of the Ocneanu graph fusion algebra, which emphasizes the chiral and ambichiral structure, can be given [14, 15, 16] in terms of tensor products over the subalgebra T . We start with an example and consider $G = D_4$. The nodes $T = \{1, 3, 4\}$ form a \mathbb{Z}_3 subalgebra of the graph fusion algebra G corresponding to the extended chiral algebra. This gives rise to the ambichiral subalgebra of \tilde{G} . One can then construct the tensor product algebra over T

$$D_4 \otimes_{\mathbb{Z}_3} D_4 \quad (2.25)$$

The tensor product \otimes_T over T means that $a \otimes_T b \equiv a \otimes b$ for all $a, b \in G$ and $t \in T$. In D_4 for example $2 \otimes 3 = 23 \otimes 1 = 2 \otimes 1$. So this algebra has six distinct elements, $1 \otimes 1$,

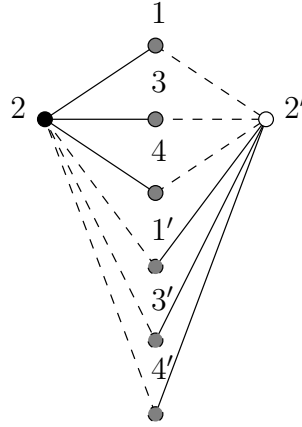


Figure 3: The Ocneanu graph \tilde{D}_4 . The nodes can be labelled by $x = (a, b)$ or (a, κ) . We have set $a = a \otimes 1$, $2' = 1 \otimes 2$ with $2 \otimes 2$ decomposed into $1', 3', 4'$. The nodes $\{1, 2, 3, 4, 1', 2', 3', 4'\}$ are alternatively labelled by $(a, \kappa) = \{(1, 1), (2, 1), (3, 1), (4, 1), (1, 2), (2, 2), (3, 2), (4, 2)\}$ respectively.

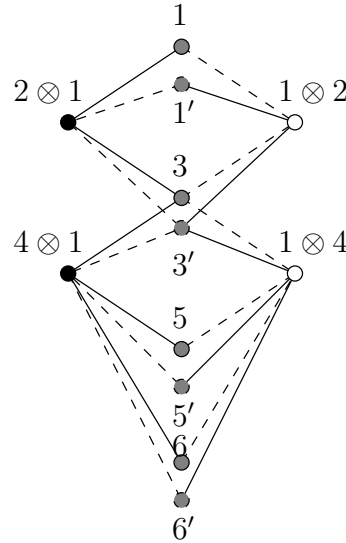


Figure 4: The Ocneanu graph $\tilde{D}_{2\ell}$ for $\ell = 3$.

$1 \otimes 2 = 3 \otimes 2 = 4 \otimes 2$, $1 \otimes 3 = 3 \otimes 1$, $1 \otimes 4 = 4 \otimes 1$, $2 \otimes 1 = 2 \otimes 3 = 2 \otimes 4$, and $2 \otimes 2$. It clearly has two generators, a left and a right, $\square_L = 2 \otimes 1$ and $\square_R = 1 \otimes 2$. They generate the *left* respectively *right chiral subalgebras*. One would like to encode this algebra in a graph as previously but there is an obstruction:

$$(2 \otimes 2)(1 \otimes 2) = 2 \otimes (1 + 3 + 4) = 2 \otimes 1 + 2 \otimes 1 + 2 \otimes 1 \quad (2.26)$$

so while there is only one edge from $2 \otimes 1$ to $2 \otimes 2 = (2 \otimes 1)(1 \otimes 2)$, there would be three in the opposite direction. This problem is solved by splitting the node $2 \otimes 2$ into three different ones, $1', 3', 4'$, using a non central extension of the algebra by an algebra of 2×2 -matrices [16]. The detail of this extension is not needed to compute twisted partition functions but we note that it leads to non-commutativity. One then obtains the graph \tilde{D}_4 presented in Fig. 3.

The same procedure works for $G = H = D_{2\ell}$ (see Fig. 4). It has a $J_{\ell+1}$ subalgebra generated by the odd vertices (the forked extremities are both taken as odd) over which the tensor square is taken and extended by an algebra of 2×2 -matrices. The result is encoded in a graph $\tilde{D}_{2\ell}$, depicted in Fig. 4, where the ambichiral $1, 3, \dots, 2\ell-3, 2\ell-1, 2\ell$ nodes are duplicated by $1', 3', \dots, (2\ell-3)', (2\ell-1)', (2\ell)'$, and where the even vertices have a left and a right counterpart $2 \otimes 1, 4 \otimes 1, \dots, 2(\ell-1) \otimes 1$ and $1 \otimes 2, 1 \otimes 4, \dots, 1 \otimes 2(\ell-1)$. The algebra structure can be worked out beginning with $1'$, which satisfies

$$\begin{aligned} 1'(1 \otimes 2) &= 2 \otimes 1, \\ 1'(2 \otimes 1) &= 1 \otimes 2, \end{aligned} \quad (2.27)$$

while $2 \otimes 2 = 1' + 3'$.

The Type I exceptional cases E_6 and E_8 are simpler as there is no need to extend the algebra. The subalgebras in these cases are generated by $T = \{1, 5, 6\}$ and $\{1, 7\}$ respectively. The A_L case is even simpler as we tensorise over the full graph algebra, yielding the same algebra back again $A_L \otimes_{A_L} A_L \simeq A_L$ so all the elements are ambichiral.

For the Type II models, $G = D_{2\ell+1}, E_7$, the Ocneanu graph algebra is defined through the square tensor of the parent theory $H = A_{4\ell-1}, D_{10}$ twisted by the involution ζ . For $G = D_{2\ell+1}$, the twisted fusion algebra is defined by $A_{4\ell-1} \otimes_{\zeta} A_{4\ell-1}$ where $a \otimes b = a\zeta(b) \otimes 1 = 1 \otimes \zeta(a)b$. It is the graph algebra of the Ocneanu graph $\tilde{D}_{2\ell+1}$ defined by $4\ell-1$ vertices forming two $A_{4\ell-1}$ graphs with plain and dashed edges, sharing the same numbering for the odd vertices (forming $\text{Exp}(D_{2\ell+1})$) but where the even ones are flipped, as pictured in Fig. 5. For $G = E_7$, the parent theory is $H = D_{10}$ and the automorphism is given by interchanging the nodes 3 and 9, so that the twist fusion algebra is $D_{10} \otimes_{T, \zeta} D_{10}$ where T is the D_{10} ambichiral subalgebra (its odd vertices, counting forked vertices as both odd). The left (right) chiral subalgebra is generated by the left (right) generator and the ambichiral subalgebra. They are both isomorphic to the primitive graph algebra H and, as in the Type I case, the ambichiral subalgebra is their intersection.

To summarize, the vertices of the Ocneanu graphs are given by distinct pairs $(a, b) \in H$ (H is the graph G or its parent graph), coding a left and a right element, or equivalently for the $D_{2\ell}$ models, a pair (a, κ) with $\kappa \in \{1, 2\}$. The twist fusion algebras just described are for the $\widehat{sl}(2)_{g-2}$ WZW theories. The Ocneanu graph fusion algebras associated with

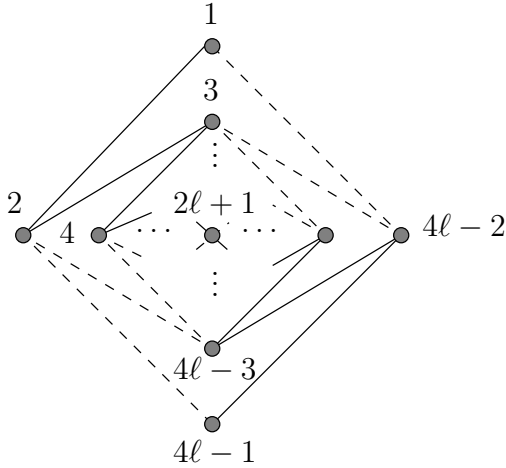


Figure 5: The Ocneanu graph $\tilde{D}_{2\ell+1}$.

A - D - E minimal models are more involved. These are given by two copies of the graph algebra $(A_{g-2}, H)/\sim$ whose vertices are pairs (r, a) with $r \in A_{h-2}$ and $a \in H$, subject to the Kac table symmetry $(r, s) \sim (g-1-r, g-s)$ if $H = A_{g-1}$ and $(r, a) \sim (g-1-r, a)$ otherwise. The vertices are, in general, labelled by $x = (r, a, b, \kappa) \in (A_{g-2}, H, H, \mathbf{Z}_2)$. In the (A_4, D_4) case for example, the Ocneanu graph is simply the tensor product of \tilde{D}_4 , the Ocneanu graph of D_4 , with the tadpole T_2 . It has three types of edges, associated with the action of the left, the right and the tadpole generators.

2.4 Twisted partition functions and extended characters

Given an A - D - E graph G , we associate to each node $a \in G$, an *extended character* $\hat{\chi}_a(q)$ which is a generating function in the modular parameter q . The ordinary characters $\chi_i(q)$ are the A -type characters. The extended characters are

$$\hat{\chi}_a(q) = \sum_{i \in A_{g-1}} n_i {}^a \chi_i(q) \quad (2.28)$$

Explicitly, in the D_4 case,

$$\hat{\chi}_1 = \chi_1 + \chi_5, \quad \hat{\chi}_2 = \chi_2 + \chi_4, \quad \hat{\chi}_3 = \hat{\chi}_4 = \chi_3. \quad (2.29)$$

We use the extended characters mostly for Type I graphs, that is, either G itself or its parent H if G is of Type II.

The twisted partition functions, which are sesquilinear combination of characters, can now be written in terms of extended characters in the following way [6, 7, 8, 16]. First, the modular invariant partition function corresponding to the unit vertex of the Ocneanu graph is associated with a sum over the subalgebra T

$$Z(q) := \sum_{a \in T} \hat{\chi}_a(q) (\hat{\chi}_{\zeta(a)}(q))^*. \quad (2.30)$$

where the automorphism ζ is the identity for the Type I models. For Type II theories, the sum over T is a sum over (a subset of) the parent graph. In the $D_{2\ell+1}$ case for example, we sum over $A_{4\ell-1}$ (they are all ambichiral). Moreover, the vertex a , associated with $\hat{\chi}_a(q)$, is paired by the twist ζ with $\hat{\chi}_{\zeta(a)}(q)^*$. It is also a sesquilinear form in terms of ordinary characters and its diagonal part gives the exponents $\text{Exp}(G)$ of Table 1. This partition function has the property of *modular invariance* in the modular parameter $q = \exp(2\pi i\tau)$, that is to say, $Z(1+\tau) = Z(\tau)$ and $Z(-1/\tau) = Z(\tau)$. The other twisted partition functions are *not* modular invariant.

The twisted partition function of other elements $a \otimes_T b$ of the Ocneanu graph, with or without an automorphism seam $\eta = \sigma^{\kappa-1}$, are obtained by the action of this element on the terms of $Z(q)$

$$Z_{a \otimes_T b}^{(\kappa)}(q) := \sum_{c \in T_\kappa} \hat{\chi}_{a c}(q) (\hat{\chi}_{\zeta(c) b}(q))^* = \sum_{c \in T_\kappa, d, e \in H} \hat{N}_{a c}{}^d \hat{N}_{b \zeta(c)}{}^e \hat{\chi}_d(q) (\hat{\chi}_e(q))^* \quad (2.31)$$

where $a c$ and $c b$ denote the product in the graph fusion algebra, that is to say, it is a linear combination of elements of the algebra and the characters are extended by linearity in their indices. The graph $H = G$ for Type I theories but is the parent graph for Type II theories. Petkova and Zuber [8] indicated that the twisted partition functions could be written in terms of the extended characters but did not write down an explicit formula. Notice that this implies that the \hat{N} structure constants involved in the calculation are all positive integers since no use is made of the graph fusion algebra for Type II models, only for the parent model which is always of Type I. For example, the action of the left generator changes the left term in $\hat{\chi}_a(q) (\hat{\chi}_{\zeta(a)}(q))^*$ to a sum over the neighbours of a in H

$$Z_{\square_L}(q) = Z_{2 \otimes 1}(q) = \sum_{a \in T} \hat{\chi}_{2 a}(q) (\hat{\chi}_{\zeta(a)}(q))^* = \sum_{a \in T, b \sim_H a} \hat{\chi}_b(q) (\hat{\chi}_{\zeta(a)}(q))^*.$$

Notice that $Z_{a \otimes_T b} = (Z_{b \otimes_T a})^*$ and, in particular for the Type I theories, the ambichiral twisted partition functions are real. A complete list of these twisted partition functions in terms of ordinary characters is given in [8, 16]. For the cases D_6 and E_6 we give a list of them in terms of extended characters in Tables 4 and 5.

The twisted partition functions just described are for the $\widehat{\mathfrak{sl}}(2)_{g-2}$, or WZW models. The twisted partition functions for the minimal models (2.23) involve pairs $(r, a) \in A_{g-2} \times H / \sim$ of indices in place of single indices $a \in H$. Here, g is the Coxeter number of H and \sim is the Kac table symmetry. The ambichiral subalgebra is the product of the two ambichiral subalgebras for each graph. In the case $(A_4, D_4) / \sim = (T_2, D_4)$, for example, the modular invariant partition function is

$$Z_1 = \sum_{x \in T} \hat{\chi}_x \hat{\chi}_x^* = \sum_{r \in \{1, 3\}, a \in \{1, 3, 4\} \subset D_4} \hat{\chi}_{r, a}^2 = \hat{\chi}_{1,1}^2 + \hat{\chi}_{3,1}^2 + \hat{\chi}_{1,3}^2 + \hat{\chi}_{3,3}^2 + \hat{\chi}_{1,4}^2 + \hat{\chi}_{3,4}^2 \quad (2.32)$$

where we have kept the labels $1 = 4$ and $2 = 3$ for $r \in T_2 = A_4 / \mathbb{Z}_2$. The other 15 twisted

partition functions are obtained by action of the twisted fusion algebra. For example,

$$Z_{(1,2)\otimes 1} = \hat{\chi}_{1,2}(\hat{\chi}_{1,1} + \hat{\chi}_{1,3} + \hat{\chi}_{1,4})^* + \hat{\chi}_{3,2}(\hat{\chi}_{3,1} + \hat{\chi}_{3,3} + \hat{\chi}_{3,4})^* \quad (2.33)$$

$$\begin{aligned} Z_{(3,1)\otimes 1} = & \hat{\chi}_{3,1}\hat{\chi}_{1,1}^* + (\hat{\chi}_{1,1} + \hat{\chi}_{3,1})\hat{\chi}_{3,1}^* + \hat{\chi}_{3,3}\hat{\chi}_{1,3}^* + (\hat{\chi}_{1,3} + \hat{\chi}_{3,3})\hat{\chi}_{3,3}^* \\ & + \hat{\chi}_{3,4}\hat{\chi}_{1,4}^* + (\hat{\chi}_{1,4} + \hat{\chi}_{3,4})\hat{\chi}_{3,4}^* \end{aligned} \quad (2.34)$$

and so on as listed in Table 6.

$$\begin{aligned} Z_1 &= \hat{\chi}_{1,1}\hat{\chi}_{1,1}^* + \hat{\chi}_{3,1}\hat{\chi}_{3,1}^* + \hat{\chi}_{1,3}\hat{\chi}_{1,3}^* + \hat{\chi}_{3,3}\hat{\chi}_{3,3}^* + \hat{\chi}_{1,4}\hat{\chi}_{1,4}^* + \hat{\chi}_{3,4}\hat{\chi}_{3,4}^* \\ Z_{\eta\otimes 1} &= \hat{\chi}_{1,2}(\hat{\chi}_{1,1} + \hat{\chi}_{1,3} + \hat{\chi}_{1,4})^* + \hat{\chi}_{3,2}(\hat{\chi}_{3,1} + \hat{\chi}_{3,3} + \hat{\chi}_{3,4})^* = Z_{1\otimes\eta}^* \\ Z_{\psi} &= \hat{\chi}_{1,3}\hat{\chi}_{1,1}^* + \hat{\chi}_{3,3}\hat{\chi}_{3,1}^* + \hat{\chi}_{1,4}\hat{\chi}_{1,3}^* + \hat{\chi}_{3,4}\hat{\chi}_{3,3}^* + \hat{\chi}_{1,1}\hat{\chi}_{1,4}^* + \hat{\chi}_{3,1}\hat{\chi}_{3,4}^* = Z_{\psi^\dagger} \\ Z_{\epsilon} &= \hat{\chi}_{3,1}\hat{\chi}_{1,1}^* + (\hat{\chi}_{1,1} + \hat{\chi}_{3,1})\hat{\chi}_{3,1}^* + \hat{\chi}_{3,3}\hat{\chi}_{1,3}^* + (\hat{\chi}_{3,3} + \hat{\chi}_{1,3})\hat{\chi}_{3,3}^* + \\ & \quad \hat{\chi}_{3,4}\hat{\chi}_{1,4}^* + (\hat{\chi}_{3,4} + \hat{\chi}_{1,4})\hat{\chi}_{3,4}^* \\ Z_{\xi\otimes 1} &= \hat{\chi}_{3,2}(\hat{\chi}_{1,1} + \hat{\chi}_{1,3} + \hat{\chi}_{1,4})^* + (\hat{\chi}_{1,2} + \hat{\chi}_{3,2})(\hat{\chi}_{3,1} + \hat{\chi}_{3,3} + \hat{\chi}_{3,4})^* = Z_{1\otimes\xi}^* \\ Z_{\sigma} &= \hat{\chi}_{1,3}\hat{\chi}_{1,1}^* + \hat{\chi}_{3,3}\hat{\chi}_{3,1}^* + \hat{\chi}_{1,4}\hat{\chi}_{1,3}^* + \hat{\chi}_{3,4}\hat{\chi}_{3,3}^* + \hat{\chi}_{1,1}\hat{\chi}_{1,4}^* + \hat{\chi}_{3,1}\hat{\chi}_{3,4}^* \\ &= Z_{\sigma^\dagger} \\ Z_{1'} &= |\hat{\chi}_{1,2}|^2 + |\hat{\chi}_{3,2}|^2 = Z_{\psi'} = Z_{\psi^{\dagger'}} \\ Z_{\epsilon'} &= \hat{\chi}_{1,2}\hat{\chi}_{3,2}^* + \hat{\chi}_{3,2}\hat{\chi}_{1,2}^* + |\hat{\chi}_{3,2}|^2 = Z_{\sigma'} = Z_{\sigma^{\dagger'}} \\ \hat{\chi}_{r,1} &:= \chi_{r,1} + \chi_{r,5}, \quad \hat{\chi}_{r,2} := \chi_{r,2} + \chi_{r,4}, \quad \hat{\chi}_{r,3} = \hat{\chi}_{r,4} := \chi_{r,3}. \end{aligned}$$

Table 6: The (A_4, D_4) twisted partition functions of the 3-state Potts model. The extended characters are given in terms of the Virasoro minimal characters $\chi_{r,s}$.

3 Lattice Realization of Twisted Boundary Conditions

3.1 A - D - E lattice models

A solvable [17] A - D - E lattice model [11, 18] is associated with a graph G , of A , D or E type. We place spins on the sites of the square lattice, where the spin states are taken to be the nodes of the graph G and neighbouring sites on the lattice must be neighbouring nodes on the graph. The probability distribution of spins is defined by the critical (unfused) Boltzmann weight of each face (or plaquette) of spins, depending on a spectral parameter u . For four spins $a, b, c, d \in G$ such that $(a, b), (b, c), (c, d), (d, a)$ are pairs of neighbours in G , the Boltzmann weight is

$$W^{11} \left(\begin{array}{cc} d & c \\ a & b \end{array} \middle| u \right) = \frac{d}{a} \boxed{u}^c_b = s(\lambda - u) \delta_{ac} + s(u) \sqrt{\frac{\psi_a \psi_c}{\psi_b \psi_d}} \delta_{bd} \quad (3.1)$$

and zero otherwise. Here, g is the Coxeter number of G , $\lambda = \frac{\pi}{g}$, $s(u) = \frac{\sin(u)}{\sin(\lambda)}$ and ψ_a is the entry, associated with the node a , of the Perron-Frobenius eigenvector of the adjacency matrix G .

These Boltzmann weights can be represented [4] by a local face operator $X_j(u)$

$$X_j(u) = \begin{array}{c} \text{diamond} \\ \text{---} \\ u \\ \text{---} \\ \text{---} \end{array} = s(\lambda - u)I + s(u)e_j \quad (3.2)$$

$j-1 \quad j \quad j+1$

in the Temperley-Lieb algebra $\mathcal{T}(N, \lambda)$

$$\begin{aligned} e_j^2 &= s(2\lambda) e_j \\ e_j e_k e_j &= e_j, \quad |j - k| = 1 \\ e_j e_k &= e_k e_j, \quad |j - k| > 1 \end{aligned} \quad (3.3)$$

where $e_j = X_j(\lambda)$ is a Temperley-Lieb generator and j is an integer labelling the N positions along a row of the lattice.

3.2 Fusion projectors

Each of the A - D - E models gives rise to a hierarchy of *fused* models whose Boltzmann weights we are going to describe. They are associated with *blocks* of faces where the internal spins are summed over in a particular way.

We first define recursively the fusion operators P_j^r , for $r = 1, 2, \dots, g$ as follows

$$\begin{aligned} P_j^1 &= P_j^2 = I \\ P_j^r &= \frac{1}{S_{r-1}} P_{j+1}^{r-1} X_j(-(r-2)\lambda) P_{j+1}^{r-1}, \quad r \geq 3, \end{aligned} \quad (3.4)$$

where $S_k = s(k\lambda)$ and j is appropriately restricted [4]. Thus, P_j^r can be expressed as a function of $e_j, e_{j+1}, \dots, e_{j+(r-3)}$. In particular,

$$P_j^3 = \frac{1}{S_2} \begin{array}{c} \text{diamond} \\ \text{---} \\ -\lambda \\ \text{---} \\ \text{---} \end{array} = I - \frac{1}{S_2} \begin{array}{c} \text{diamond} \\ \text{---} \\ +\lambda \\ \text{---} \\ \text{---} \end{array}. \quad (3.5)$$

We shall represent the fusion operators diagrammatically as

$$P_j^r = \begin{array}{c} \text{---} \\ \text{---} \\ \text{---} \\ \text{---} \\ \text{---} \\ \text{---} \end{array} \quad (3.6)$$

$j-1 \quad j \quad j+r-3 \quad j+r-2$

It is easy to show that this operator is in fact a projector. Moreover,

$$P_{j'}^{r'} P_j^r = P_j^r P_{j'}^{r'} = P_j^r, \quad \text{for } 0 \leq j' - j \leq r - r'. \quad (3.7)$$

$$\begin{array}{c} \text{---} \\ \text{---} \\ \text{---} \\ \text{---} \\ \text{---} \\ \text{---} \end{array} = \begin{array}{c} \text{---} \\ \text{---} \\ \text{---} \\ \text{---} \\ \text{---} \\ \text{---} \end{array}.$$

In particular, the local face operator $\begin{array}{c} \diamond \\ \swarrow \searrow \\ +\lambda \end{array} = S_2 e_j$ is a projector orthogonal to all the $P_{j'}^r$ for $0 \leq j - j' \leq r - 3$. This fact is a defining property of the orthogonal projector P_j^r

$$\text{Im } P_j^r = \bigcap_{k=j}^{j+r-3} \text{Ker } e_k. \quad (3.8)$$

Clearly, we can decompose the projector P_j^r onto the space of paths with given end points: $P^r(a, b)$ is the fusion projector acting on paths from a to b in $r-1$ steps. Its rank is given by the fused adjacency matrix entries

$$\text{Rank}(P^r(a, b)) = n_r a^b. \quad (3.9)$$

The $+1$ eigenvectors of $P^r(a, b)$ are thus indexed by an integer $\gamma = 1, 2, \dots, n_r a^b$ referred to as the *bond variable*. We denote these eigenvectors by $\mathbf{U}_\gamma^r(a, b)$ and call them *fusion vectors* or *essential paths*. Explicitly, in the representation (3.1) of the Temperley-Lieb algebra $\mathcal{T}(r-2, \lambda)$, these generators act on the paths from a to b in $r-1$ steps as

$$e_k(a_0, a_1, \dots, a_{k-1}, a_k, a_{k+1}, \dots, a_{r-2}, b) = \sum_{\substack{\delta_{a_{k-1}, a_{k+1}} \\ c \sim a_{k-1}}} \frac{\psi_{a_k}^{1/2} \psi_c^{1/2}}{\psi_{a_{k-1}}^{1/2} \psi_{a_{k+1}}^{1/2}} (a_0, a_1, \dots, a_{k-1}, c, a_{k+1}, \dots, a_{r-2}, b). \quad (3.10)$$

In the D and E cases multiplicities occur and there is some freedom in the choice of fusion vectors corresponding to a unitary change of basis. In the A_L case, however, there is a unique fusion path. As an example, there are two paths on A_L , going from the node 2 to itself in 2 steps, namely $(2, 1, 2)$ and $(2, 3, 2)$. As they both backtrack, the fusion vector $\mathbf{U}_1^3(2, 2)$ is unique, proportional to their difference $\psi_3^{1/2}(2, 1, 2) - \psi_1^{1/2}(2, 3, 2)$ and the fused adjacency matrix entry is $n_{32}^2 = 1$. In the D_4 case, there is the path $(2, 4, 2)$ as well, so that there are two linearly independent fusion vectors, the previous one and $(2, 3, 2) - (2, 4, 2)$ or any similar linear combination (notice that $\psi_3 = \psi_4$). The fused adjacency matrix has a two as the corresponding entry $n_{32}^2 = 2$. The general form of the unique A_L fusion vector at fusion level $s \leq L$ between the vertex 2 and the vertex $s-1$ is given by the following formula of cancelling alternating backtracking paths, generalizing the one just described for $s=3$

$$\begin{aligned} \mathbf{U}_1^s(2, s-1) = & \left(\psi_1^{-1/2} \psi_2^{-1/2}(2, 1, 2, 3, \dots, s-1) - \psi_2^{-1/2} \psi_3^{-1/2}(2, 3, 2, 3, \dots, s-1) \right. \\ & \left. + \psi_3^{-1/2} \psi_4^{-1/2}(2, 3, 4, 3, \dots, s-1) + \dots + (-1)^s \psi_{s-1}^{-1/2} \psi_s^{-1/2}(2, \dots, s-1, s, s-1) \right) \end{aligned} \quad (3.11)$$

and similarly for D_ℓ with fusion level $s < \ell-1$. But at fusion level $s = \ell-1$, the fork gives rise to a two dimensional space of fusion vectors. One choice of orthonormal basis is given (with ν the appropriate normalisation constant) by

$$\begin{aligned} \mathbf{U}_1^{\ell-1}(2, \ell-2) = & \frac{1}{\nu} \left(\psi_1^{-1/2} \psi_2^{-1/2}(2, 1, 2, 3, \dots, \ell-2) - \psi_2^{-1/2} \psi_3^{-1/2}(2, 3, 2, 3, \dots, \ell-2) \right. \\ & \left. + \psi_3^{-1/2} \psi_4^{-1/2}(2, 3, 4, 3, \dots, \ell-2) + \dots \right. \\ & \left. + \frac{1}{2} (-1)^{\ell-1} \psi_{\ell-2}^{-1/2} \psi_{\ell-1}^{-1/2}(2, \dots, \ell-2, \ell-1, \ell-2) + \frac{1}{2} (-1)^{\ell-1} \psi_{\ell-2}^{-1/2} \psi_s^{-1/2}(2, \dots, \ell-2, \ell, \ell-2) \right), \\ \mathbf{U}_2^{\ell-1}(2, \ell-2) = & \frac{1}{\sqrt{2}} \left((2, \dots, \ell-2, \ell-1, \ell-2) - (2, \dots, \ell-2, \ell, \ell-2) \right). \end{aligned} \quad (3.12)$$

3.3 Fused face operators

The fusion projectors allow us to define the (p, q) -fused face operators consisting of q rows of p local face operators with relative shifts in the spectral parameter by $\pm\lambda$ from one face to the next

$$X_j^{pq}(u) = \begin{array}{c} \text{Diagram showing a single fused face operator } X^{pq}(u) \text{ with indices } j-1, j+q-1, j+p+q-2 \text{ and top index } j+p-1. \end{array} = \begin{array}{c} \text{Diagram showing the fused operator } X^{pq}(u) \text{ as a stack of } p \text{ horizontal layers, each with a projector } P_j^{q+1} \text{ and } P_{j+q}^{p+1}, \text{ with spectral parameters } u+(q-p)\lambda, u+(q-1)\lambda, u, u-(p-1)\lambda. \end{array} . \quad (3.13)$$

The position of the projectors and spectral parameters can be altered by *pushing-through*

$$X_j^{pq}(u) = \begin{array}{c} \text{Diagram showing the fused operator } X^{pq}(u) \text{ with projectors } P_{j+p}^{q+1} \text{ and } P_{j+q}^{p+1} \text{ and spectral parameters } u-(p-1)\lambda, u+(q-p)\lambda. \end{array} = \begin{array}{c} \text{Diagram showing the fused operator } X^{pq}(u) \text{ with projectors } P_j^{p+1} \text{ and } P_{j+q}^{q+1} \text{ and spectral parameters } u, u+(q-1)\lambda. \end{array} = \begin{array}{c} \text{Diagram showing the fused operator } X^{pq}(u) \text{ with projectors } P_j^{p+1} \text{ and } P_j^{q+1} \text{ and spectral parameters } u. \end{array} . \quad (3.14)$$

These properties imply several others, namely the *Transposition Symmetry*

$$X_j^{pq}(u)^T = X_j^{qp}(u + (q-p)\lambda) \quad (3.15)$$

the *Generalized Yang-Baxter Equation* (GYBE)

$$\begin{array}{c} \text{Diagram showing the GYBE relation between three fused face operators } X^{qp}(v), X^{qq'}(u+v), X^{pq'}(u) \text{ and } X^{qq'}(u+v), X^{qp}(v), X^{pq'}(u). \end{array} = \begin{array}{c} \text{Diagram showing the GYBE relation between three fused face operators } X^{qq'}(u+v), X^{qp}(v), X^{pq'}(u) \text{ and } X^{qq'}(u+v), X^{qp}(v), X^{pq'}(u). \end{array} . \quad (3.16)$$

the *Inversion Relation*

$$X_j^{pq}(u) X_j^{qp}(-u) = \dots \begin{array}{c} \text{Diagram showing the inversion relation between fused face operators } X^{pq}(u) \text{ and } X^{qp}(-u). \end{array} \dots = s_1^{pq}(u) s_1^{pq}(-u) P_j^{q+1} P_{j+q}^{p+1} \quad (3.17)$$

where $s_i^{pq}(u) = \prod_{j=0}^{p-1} \prod_{k=0}^{q-1} s(u + (i-j+k)\lambda)$ (we will also use the notation s_i^p for $q = 1$) and the *Abelian Property*

$$X_j^{pq}(u + (p-1)\lambda) X_j^{qp}(v + (q-1)\lambda) = X_j^{pq}(v + (p-1)\lambda) X_j^{qp}(u + (q-1)\lambda) .$$

The braid limits of the fused face operators are

$$X_j^{pq}(i\epsilon\infty) := \lim_{u \rightarrow i\epsilon\infty} \frac{e^{-i\epsilon\frac{(g+1)pq}{2}\lambda}}{s_0^{1q}(u) s_{-1}^{p-1q}(u)} X_j^{pq}(u), \quad \epsilon = \pm 1 \quad (3.18)$$

It follows that

$$X_j^{pq}(+i\infty) = X_j^{pq}(-i\infty)^* \quad (3.19)$$

and the inversion relation becomes

$$X_j^{pq}(i\epsilon\infty) X_j^{pq}(i\epsilon\infty)^\dagger = P_j^{q+1} P_{j+q}^{p+1} \quad (3.20)$$

so that these operators are unitary.

The fused face operators, contracted against the fusion vectors, yield the (p, q) -fused Boltzmann weights which depend not only on the spins at the four corners but also on the bond variables on the edges

$$W^{pq} \left(\begin{array}{ccc|c} d & \gamma & c & \\ \delta & & \beta & \\ a & \alpha & b & \end{array} \middle| u \right) = \begin{array}{c} d \quad \gamma \quad c \\ \delta \quad u \quad \beta \\ a \quad \alpha \quad b \end{array} = \frac{1}{s_0^{p,q-1}(u)} \mathbf{U}_\delta^{q-1}(d,a) \begin{array}{c} d \quad \mathbf{U}_\gamma^{p-1}(d,c)^\dagger \quad c \\ \downarrow \quad X^{pq}(u) \quad \mathbf{U}_\beta^{q-1}(c,b)^\dagger \\ a \quad \mathbf{U}_\alpha^{p-1}(a,b) \quad b \end{array} \quad (3.21)$$

where the function $s_0^{p,q-1}(u)$ eliminates some scalar factors common to all the spin configurations which appear in the process of fusion. In the A_L case the bond variables are redundant. The fused Boltzmann weights satisfy the reflection symmetry

$$W^{pq} \left(\begin{array}{ccc|c} d & \gamma & c & \\ \delta & & \beta & \\ a & \alpha & b & \end{array} \middle| u \right) = \frac{s_0^{q,p-1}(u)}{s_0^{p,q-1}(u)} W^{qp} \left(\begin{array}{ccc|c} d & \delta & a & \\ \gamma & & \alpha & \\ c & \beta & b & \end{array} \middle| u + (q-p)\lambda \right) \quad (3.22)$$

and *Crossing Symmetry*

$$W^{pq} \left(\begin{array}{ccc|c} d & \gamma & c & \\ \delta & & \beta & \\ a & \alpha & b & \end{array} \middle| u \right) = \sqrt{\frac{\psi_a \psi_c}{\psi_b \psi_d}} \frac{s_0^{q,p-1}(\lambda-u)}{s_0^{p,q-1}(u)} W^{qp} \left(\begin{array}{ccc|c} a & \delta & d & \\ \alpha & & \gamma & \\ b & \beta & c & \end{array} \middle| \lambda-u \right). \quad (3.23)$$

We use these fused Boltzmann weights to construct commuting transfer matrices with seams.

3.4 Integrable seams on the torus

Simple integrable seams are modified faces. Surprisingly, they produce some new twisted boundary conditions even for the Ising model [19, 20]. They come in four different types, r , s , a and η -type where $r \in A_{g-2}$, $s \in A_{g-1}$, $a \in H$ and $\eta \in \Gamma$. Here $H = G$ for Type I theories and is the parent for Type II theories. A composite integrable seam x consists of several simple seams glued together with four spins c, d, e, f at the corners. The integrable

seams $x = (r, a, b, \sigma^{\kappa-1})$ give rise to the conformal seams (r, a, b, κ) in the continuum scaling limit. The adjacency matrix of an integrable seam $x = (r, a, b, \sigma^{\kappa-1})$ is given by

$$\tilde{n}_x = \begin{cases} n_r \hat{N}_a \hat{N}_b \sigma^{k-1}, & G \text{ of Type I} \\ n_r n_a^{(G H)} n_b^{(G H)} \sigma^{k-1}, & G \text{ of Type II and } x \neq (r, X) \\ n_r n_2^{(G H)} (n_6^{(G H)} - n_4^{(G H)}), & G = E_7 \text{ and } x = (r, X) \end{cases} \quad (3.24)$$

where $n_a^{(G H)}$ with $a \in H$ are the intertwiners [3] of G relative to H

$$n_{ab}^{(G H)c} = \sum_{m \in \text{Exp}(G)} \frac{\psi_a^{(H)m}}{\psi_1^{(H)m}} \psi_b^{(G)m} \psi_c^{(G)m*} \quad (3.25)$$

and X is the special node [8] of the E_7 Ocneanu graph. The matrices $(\tilde{n}_x)_c^d$ and $(\tilde{n}_x)_f^e$ encode the allowed adjacency between spins c, d at the bottom and f, e at the top of a composite seam. Although our interpretation of these matrices is different, these matrices coincide exactly with the \tilde{n}_x matrices of Petkova and Zuber. Our definition, however, is intrinsic to the seam and we do not need to invoke boundary conditions on the cylinder. The matrices \tilde{n}_x form a (non-faithful) representation of the Ocneanu graph fusion algebra

$$\tilde{n}_x \tilde{n}_y = \sum_z \tilde{N}_{xy}^z \tilde{n}_z \quad (3.26)$$

We consider composite seams of type $x = (r, s, \eta)$ and first define $W_{(r,1,1)}^q$, the r -type seam for the (p, q) -fused model. It is a usual $(r-1, q)$ -fused face (it doesn't depend on the horizontal fusion level p) with an extra parameter ξ acting as a shift in the spectral parameter, and another choice for the removal of common scalar factors

$$W_{(r,1,1)}^q \left(\begin{array}{ccc} d & \gamma & c \\ \delta & & \beta \\ a & \alpha & b \end{array} \middle| u, \xi \right) = \frac{s_0^{r-1} q^{-1} (u + \xi)}{s_{-1}^{r-2} q (u + \xi)} W^{(r-1)q} \left(\begin{array}{ccc} d & \gamma & c \\ \delta & & \beta \\ a & \alpha & b \end{array} \middle| u + \xi \right). \quad (3.27)$$

An s -type seam with $s \in A_{g-1}$ is the normalized *braid limit* of an r -type seam, it does not depend on the spectral parameter

$$W_{(1,s,1)}^q \left(\begin{array}{ccc} d & \gamma & c \\ \delta & & \beta \\ a & \alpha & b \end{array} \right) = \lim_{\xi \rightarrow i\infty} \frac{e^{-i \frac{(g+1)(s-1)q}{2} \lambda}}{s_0^{1q} (u + \xi)} W_{(s,1)}^q \left(\begin{array}{ccc} d & \gamma & c \\ \delta & & \beta \\ a & \alpha & b \end{array} \middle| u, \xi \right). \quad (3.28)$$

In general the s -type weights are complex. The complex conjugate gives the weights in the other braid limit $\xi \rightarrow -i\infty$. By the reflection and crossing symmetries (3.22) and (3.23)

$$W_{(1,s,1)}^q \left(\begin{array}{ccc} d & \gamma & c \\ \delta & & \beta \\ a & \alpha & b \end{array} \right) = \sqrt{\frac{\psi_a \psi_c}{\psi_b \psi_d}} W_{(1,s,1)}^q \left(\begin{array}{ccc} a & \alpha & b \\ \delta & & \beta \\ d & \gamma & c \end{array} \right)^* \quad (3.29)$$

These braid-limit face weights provide us with a representation of the braid group.

It is known [21, 22] that discrete symmetries play an important role in twisted boundary conditions. In fact, there is an integrable seam corresponding to each discrete symmetry.

Specifically, the graph automorphisms $\eta \in \Gamma$, satisfying $G_{a,b} = G_{\eta(a),\eta(b)}$, leave the face weights invariant

$$W^{pq} \begin{pmatrix} d & \gamma & c \\ \delta & & \beta \\ a & \alpha & b \end{pmatrix} \Big| u = \begin{array}{c} d \quad \gamma \quad c \\ \delta \quad \beta \\ a \quad \alpha \quad b \end{array} = \begin{array}{c} \eta(d) \quad \gamma \quad \eta(c) \\ \delta \quad \beta \\ \eta(a) \quad \eta(b) \end{array} = W^{pq} \begin{pmatrix} \eta(d) & \gamma & \eta(c) \\ \delta & & \beta \\ \eta(a) & \alpha & \eta(b) \end{pmatrix} \Big| u \quad (3.30)$$

and act through the special seam [23]

$$W_{(1,1,\eta)}^q \begin{pmatrix} d & c \\ \alpha & \beta \\ a & b \end{pmatrix} = \delta_{b\eta(a)} \delta_{c\eta(d)} \begin{array}{c} d \quad \eta(d) \\ \alpha \quad \beta \\ a \quad \eta(a) \end{array} = \begin{cases} 1, & n_{q+1}{}^a \neq 0, \alpha = \beta \\ & b = \eta(a), c = \eta(d), \\ 0, & \text{otherwise.} \end{cases} \quad (3.31)$$

Notice that the $(r, s, \eta) = (1, 1, 1)$ seam, where $\eta = 1$ denotes the identity automorphism, is the empty seam

$$W_{(1,1,1)}^q \begin{pmatrix} d & c \\ \alpha & \beta \\ a & b \end{pmatrix} = \delta_{ab} \delta_{cd} \delta_{\alpha\beta} n_{q+1}{}^c. \quad (3.32)$$

The push-through property is also satisfied for an η -type seam.

3.5 Construction of a -type seams for Type I theories

In this section we construct a new type of fusion for Type I models labelled by the nodes $a \in G$. The fused Boltzmann weights giving the $(1, a)$ -seams are obtained in the braid limits $u \rightarrow i\epsilon\infty$ with $\epsilon = \pm 1$ and are independent of the spectral parameter u . This new type of fusion is associated to the \hat{N}_a graph fusion matrices in exactly the same way as the usual fusions are associated to the fused adjacency matrices n_s . For Type II models, the construction is applied to the parent Type I graphs in the next section. Previously, all known fusions were labelled by Young tableaux. In our case, r and s label $sl(2)$ tableaux with r or s boxes in a single row. The construction of fusions labelled by nodes of graphs is an important step in understanding the graph fusion algebras associated with integrable and conformal seams.

In constructing the a -type seams in this section we focus on vertically unfused face weights with $q = 1$. Recall that the s -type seams are the braid limit of the $(s - 1)$ fused Boltzmann weights which are obtained by acting with the fusion projector P_j^s on the face operators $X_j(u)$. From (3.9) we see that the admissible spins at the corners of the $(s - 1)$ fused face weights and the number of horizontal bond variables are given by the non-zero entries in the fused adjacency matrices n_s with $s \in A_{g-1}$. From Section 2.2, these fused adjacency matrices are linear combinations of the graph fusion matrices

$$n_s = \sum_{a \in G} n_{s1}{}^a \hat{N}_a \quad (3.33)$$

This motivates us to define a new type of fusion projector $\hat{P}_j^{(s)a}(b, c)$ associated with \hat{N}_a and acting on paths between b and c by orthonormally decomposing the s -type projector $P_j^s(b, c)$

$$P_j^s(b, c) = \sum_{a \in G} n_{s1}{}^a \hat{P}_j^{(s)a}(b, c) \quad (3.34)$$

where each of the \hat{N}_a fusion projectors $\hat{P}_j^{(s)a}(b, c)$ separately satisfies the *push-through property* (3.14) *in the braid limit*. These projectors $\hat{P}^{(s)a}(b, c)$ which may have complex entries are required to satisfy

$$1. \text{ Decomposition: } P^s(b, c) = \sum_{a \in G} n_{s1}^a \hat{P}^{(s)a}(b, c) \quad (3.35)$$

$$2. \text{ Orthogonality: } \hat{P}^{(s)a}(b, c) \hat{P}^{(s)f}(b, c) = 0, \quad a \neq f, \quad (3.36)$$

$$3. \text{ Projection: } \hat{P}^{(s)a}(b, c)^2 = \hat{P}^{(s)a}(b, c), \quad \hat{P}^{(s)a}(b, c)^\dagger = \hat{P}^{(s)a}(b, c) \quad (3.37)$$

$$4. \text{ Adjacency: } \text{Rank}(\hat{P}^{(s)a}(b, c)) = \hat{N}_{ab}^c \quad (3.38)$$

By the above conditions (3.35)-(3.38), $P^s(b, c)$ and $\{\hat{P}^{(s)a}(b, c)\}_{a \in G}$ are simultaneously diagonalizable with a common set of eigenvectors. It follows that $P^{(s)a}(b, c)$ can be decomposed as

$$\hat{P}^{(s)a}(b, c) = \sum_{\mu=1}^{\hat{N}_{ab}^c} \hat{\mathbf{U}}_\mu^{(s)a}(b, c) \hat{\mathbf{U}}_\mu^{(s)a}(b, c)^\dagger \quad (3.39)$$

where $\hat{\mathbf{U}}_\mu^{(s)a}(b, c)$ are the simultaneous eigenvectors of $P^s(b, c)$ and $\{\hat{P}^{(s)a}(b, c)\}_{a \in G}$ satisfying

$$\begin{aligned} P^s(b, c) \hat{\mathbf{U}}_\mu^{(s)a}(b, c) &= \hat{P}^{(s)a}(b, c) \hat{\mathbf{U}}_\mu^{(s)a}(b, c) = \hat{\mathbf{U}}_\mu^{(s)a}(b, c); \\ \hat{P}^{(s)f}(b, c) \hat{\mathbf{U}}_\mu^{(s)a}(b, c) &= \mathbf{0}, \quad a \neq f. \end{aligned} \quad (3.40)$$

Thus, the construction of the new type of fusion at $u \rightarrow i\epsilon\infty$, with $\epsilon = \pm 1$, is equivalent to finding the appropriate orthonormal basis for the fusion vectors $\{\hat{\mathbf{U}}_{\epsilon\mu}^{(s)a}(b, c)\}$ of $P^s(b, c)$ satisfying the conditions

$$\begin{array}{c} e \quad \hat{\mathbf{U}}_{\epsilon\nu}^{(s)f}(e, d)^\dagger \\ \boxed{X^{(s-1)1}(i\epsilon\infty)} \\ b \quad \hat{\mathbf{U}}_{\epsilon\mu}^{(s)a}(b, c) \end{array} = 0 \quad \text{for all } \mu, \nu, a \neq f, \hat{N}_{ab}^c, \hat{N}_{be}^d \neq 0 \quad (3.41)$$

which follows from the push-through property and the orthogonality of $\hat{P}_j^{(s)a}$ (3.36). Note that the \hat{N}_a fusion vectors at $u \rightarrow i\epsilon\infty$ are different for $\epsilon = +1$ and $\epsilon = -1$. By (3.19), $\hat{\mathbf{U}}_{\epsilon\mu}^{(s)a}(b, c)^*$ is the \hat{N}_a fusion vector at $u \rightarrow -i\epsilon\infty$. Hence, the \hat{N}_a fusion projectors at $u \rightarrow \pm i\infty$ are complex conjugates

$$\hat{P}_{u \rightarrow -i\infty}^{(s)a}(b, c) = \hat{P}_{u \rightarrow +i\infty}^{(s)a}(b, c)^*. \quad (3.42)$$

From now on, unless otherwise stated, the terms \hat{N}_a fusion projector and \hat{N}_a fusion vector refer to the braid limit $u \rightarrow +i\infty$. We emphasize that $\hat{P}_j^{(s)a}$ does not satisfy the push-through property if the face operator $X^{(s-1)1}(u)$ depends on u , that is, if we move away from the braid limit.

The \hat{N}_a fusion vectors can be obtained by solving (3.41). However, there is a more convenient approach taking advantage of the unitarity of the face operators in the braid limit (3.20). This provides a unitary transformation between essential paths, so that the unknown \hat{N}_a fusion vectors can be obtained from known ones by a unitary transformation.

The fusion vectors $\mathbf{U}^s(e, d)$ with $\hat{N}_{ae}^d = 1$ are automatically the same as the \hat{N}_a fusion vectors due to the adjacency condition (3.38)

$$\mathbf{U}^s(e, d) \equiv \hat{\mathbf{U}}^{(s)a}(e, d), \quad \hat{N}_{ae}^d = 1 \quad (3.43)$$

So suppose that $\hat{\mathbf{U}}_\mu^{(s)a}(e, d)$ is known for some given s, d, e . Then for any $b, c \in G$ with $\hat{N}_{ab}^c \neq 0$ satisfying

$$n_{2d}^c \neq 0 \quad \text{and} \quad n_{2e}^{b'} n_{sb'}^c = n_{sb}^c \delta_{b', b} \quad (3.44)$$

the \hat{N}_a fusion vector $\hat{\mathbf{U}}_\mu^{(s)a}(b, c)$ is given by the unitary transformation

$$\hat{\mathbf{U}}_\mu^{(s)a}(e, d) \mapsto \hat{\mathbf{U}}_\mu^{(s)a}(b, c) : \quad \hat{\mathbf{U}}_\mu^{(s)a}(b, c) = \begin{array}{c} \text{Diagram showing a unitary transformation from } \hat{\mathbf{U}}_\mu^{(s)a}(e, d) \text{ to } \hat{\mathbf{U}}_\mu^{(s)a}(b, c). \text{ The diagram is a parallelogram with vertices } e, b, c, d. \text{ The top edge } eb \text{ is labeled } b, \text{ bottom edge } cd \text{ is labeled } c, \text{ left edge } ed \text{ is labeled } d, \text{ and right edge } bc \text{ is labeled } e. \text{ The diagonal } eb \text{ is labeled } X^{(s-1)}(-i\infty) \text{ and the diagonal } cd \text{ is labeled } X^{(s-1)}(i\infty). \text{ The bottom edge } cd \text{ is labeled } \hat{\mathbf{U}}_\mu^{(s)a}(e, d). \end{array} \quad (3.45)$$

Clearly, it is a fusion vector of $P^s(b, c)$ by the push-through property of the ordinary projector. It is also an \hat{N}_a fusion vector because

$$\begin{array}{c} \text{Diagram showing the calculation of } \hat{\mathbf{U}}_\mu^{(s)a}(b, c) \text{ using the formula from (3.45). The left side shows a box with } \hat{\mathbf{U}}_\nu^{(s)f}(e, d')^\dagger \text{ and } X^{(s-1)}(i\infty) \text{ inside. The right side shows the result } \hat{\mathbf{U}}_\nu^{(s)f}(e, d)^\dagger \cdot \hat{\mathbf{U}}_\mu^{(s)a}(e, d) \delta_{d', d} = \delta_{a, f} \delta_{\mu, \nu} \delta_{d', d}. \end{array} \quad (3.46)$$

by the inversion relation (3.20), which is guaranteed to be valid by (3.44) since, for any b' adjacent to e , we have $\text{Rank}(P^{(s)a}(b', c)) = n_{sb}^c \delta_{b', b}$. Thus, the \hat{N}_a fusion vectors $\hat{\mathbf{U}}_\mu^{(s)a}(b, c)$ are determined uniquely up to a phase factor and unitary gauge transformations within blocks given by $\hat{N}_{ab}^c > 1$. To be consistent, one should check that (3.45) satisfies (3.41) for all the other admissible spins. By the crossing symmetry (3.23) and (3.19), (3.45) can be expressed as the linear combination of ordinary fusion vectors

$$\hat{\mathbf{U}}_\mu^{(s)a}(b, c) = \sum_\gamma \sqrt{\frac{\psi_d \psi_b}{\psi_e \psi_c}} W_{(1, s, 1)} \begin{pmatrix} b & \gamma & c \\ e & \mu & d \end{pmatrix} \mathbf{U}_\gamma^s(b, c). \quad (3.47)$$

We now illustrate the calculations of \hat{N}_a fusion vectors for the case $G = E_6$. In E_6 , $n_s = \hat{N}_s$ for $1 \leq s \leq 3$, so it remains to find the \hat{N}_a fusion vectors for \hat{N}_4 , \hat{N}_5 and \hat{N}_6 . First, n_4 can be decomposed into \hat{N}_4 and \hat{N}_6

$$n_4 = \begin{pmatrix} 0 & 0 & 0 & 1 & 0 & 1 \\ 0 & 0 & 2 & 0 & 1 & 0 \\ 0 & 2 & 0 & 2 & 0 & 1 \\ 1 & 0 & 2 & 0 & 0 & 0 \\ 0 & 1 & 0 & 0 & 0 & 1 \\ 1 & 0 & 1 & 0 & 0 & 0 \end{pmatrix} = \begin{pmatrix} 0 & 0 & 0 & 1 & 0 & 0 \\ 0 & 0 & 1 & 0 & 1 & 0 \\ 0 & 1 & 0 & 1 & 0 & 1 \\ 1 & 0 & 1 & 0 & 0 & 0 \\ 0 & 1 & 0 & 0 & 0 & 0 \\ 0 & 0 & 1 & 0 & 0 & 0 \end{pmatrix} + \begin{pmatrix} 0 & 0 & 0 & 0 & 0 & 1 \\ 0 & 0 & 1 & 0 & 0 & 0 \\ 0 & 1 & 0 & 1 & 0 & 0 \\ 0 & 0 & 1 & 0 & 0 & 0 \\ 0 & 0 & 0 & 0 & 0 & 1 \\ 1 & 0 & 0 & 0 & 1 & 0 \end{pmatrix} = \hat{N}_4 + \hat{N}_6 \quad (3.48)$$

and only the \hat{N}_a fusion vectors for $(b, c) = (2, 3), (3, 2), (3, 4), (4, 3)$ need to be determined.

Consider $(b, c) = (2, 3)$. By (3.44), $\hat{\mathbf{U}}^{(4)4}(1, 4) \mapsto \hat{\mathbf{U}}^{(4)4}(2, 3)$ so it follows from (3.47) that

$$\hat{\mathbf{U}}^{(4)4}(2, 3) = \sum_{\gamma} \sqrt{\frac{\psi_4 \psi_2}{\psi_1 \psi_3}} W_{(1,4,1)} \begin{pmatrix} 2 & \gamma & 3 \\ 1 & 1 & 4 \end{pmatrix} \mathbf{U}_{\gamma}^4(2, 3) \quad (3.49)$$

and similarly $\hat{\mathbf{U}}^{(4)6}(1, 6) \mapsto \hat{\mathbf{U}}^{(4)6}(2, 3)$. For $(b, c) = (3, 2)$, $\{\hat{\mathbf{U}}^{(4)4}(2, 3), \hat{\mathbf{U}}^{(4)6}(2, 3)\} \mapsto \{\hat{\mathbf{U}}^{(4)4}(3, 2), \hat{\mathbf{U}}^{(4)6}(3, 2)\}$, so $\hat{\mathbf{U}}^{(4)4}(3, 2)$ is obtained by applying (3.45) to (3.49)

$$\hat{\mathbf{U}}^{(4)4}(3, 2) = \sum_{\gamma} \frac{\psi_3}{\psi_2} W_{(1,4,1)} \begin{pmatrix} 3 & \gamma & 2 \\ 2 & \hat{4} & 3 \end{pmatrix} \mathbf{U}_{\gamma}^4(3, 2) \quad (3.50)$$

where

$$W_{(1,4,1)} \begin{pmatrix} 3 & \gamma & 2 \\ 2 & \hat{4} & 3 \end{pmatrix} = \sum_{\alpha} \mathbf{U}_{\alpha}^4(2, 3)^{\dagger} \cdot \hat{\mathbf{U}}^{(4)4}(2, 3) W_{(1,4,1)} \begin{pmatrix} 3 & \gamma & 2 \\ 2 & \alpha & 3 \end{pmatrix} \quad (3.51)$$

$$= \sum_{\alpha} \sqrt{\frac{\psi_4 \psi_2}{\psi_1 \psi_3}} W_{(1,4,1)} \begin{pmatrix} 2 & \alpha & 3 \\ 1 & 1 & 4 \end{pmatrix} W_{(1,4,1)} \begin{pmatrix} 3 & \gamma & 2 \\ 2 & \alpha & 3 \end{pmatrix} \quad (3.52)$$

is the s -type seam with the bond variable $\hat{4}$ specifically chosen so that the corresponding fusion vector between $(2, 3)$ is \hat{N}_4 . Similarly we obtain $\hat{\mathbf{U}}^{(4)6}(3, 2)$. For the other cases, we apply the same procedure

$$\begin{aligned} \{\hat{\mathbf{U}}^{(4)4}(6, 3), \hat{\mathbf{U}}^{(4)6}(6, 5)\} &\mapsto \{\hat{\mathbf{U}}^{(4)4}(3, 4), \hat{\mathbf{U}}^{(4)6}(3, 4)\} \\ \{\hat{\mathbf{U}}^{(4)4}(5, 2), \hat{\mathbf{U}}^{(4)6}(5, 6)\} &\mapsto \{\hat{\mathbf{U}}^{(4)4}(4, 3), \hat{\mathbf{U}}^{(4)6}(4, 3)\} \end{aligned} \quad (3.53)$$

Finally, we repeat the whole process for $n_5 = \hat{N}_3 + \hat{N}_5$ to obtain the \hat{N}_5 fusion vectors.

In summary, the \hat{N}_a fusion vectors for E_6 derived from n_4 and n_5 are listed below in terms of the given path basis with $\lambda = \pi/12$.

For $n_4 = \hat{N}_4 + \hat{N}_6$:

$$\begin{aligned} (2, 3) \text{ Basis: } & \{(2, 1, 2, 3), (2, 3, 2, 3), (2, 3, 4, 3), (2, 3, 6, 3)\} \\ \hat{\mathbf{U}}^{(4)4}(2, 3) &= \frac{\sqrt{3}-1}{2} \left((\sqrt{3}+1)^{1/2} e^{-\frac{7\lambda}{2}i}, -e^{-\frac{7\lambda}{2}i}, e^{\frac{5\lambda}{2}i}, -(\sqrt{3}+1)^{1/2} e^{\frac{11\lambda}{2}i} \right) \\ \hat{\mathbf{U}}^{(4)6}(2, 3) &= \frac{\sqrt{3}-1}{2} \left(\sqrt{2} e^{-\frac{7\lambda}{2}i}, -(\sqrt{3}-1)^{1/2} e^{-\frac{7\lambda}{2}i}, -(\sqrt{3}+1)^{1/2} e^{\frac{11\lambda}{2}i}, \sqrt{2} e^{\frac{7\lambda}{2}i} \right) \end{aligned} \quad (3.54)$$

$$\begin{aligned} (3, 2) \text{ Basis: } & \{(3, 2, 1, 2), (3, 2, 3, 2), (3, 4, 3, 2), (3, 6, 3, 2)\} \\ \hat{\mathbf{U}}^{(4)4}(3, 2) &= \frac{\sqrt{3}-1}{2} \left(-(\sqrt{3}+1)^{1/2} e^{5\lambda i}, e^{5\lambda i}, -e^{-\lambda i}, (\sqrt{3}+1)^{1/2} e^{-4\lambda i} \right) \\ \hat{\mathbf{U}}^{(4)6}(3, 2) &= \frac{\sqrt{3}-1}{2} \left(-\sqrt{2} e^{5\lambda i}, (\sqrt{3}-1)^{1/2} e^{5\lambda i}, (\sqrt{3}+1)^{1/2} e^{-4\lambda i}, -\sqrt{2} e^{-2\lambda i} \right) \end{aligned} \quad (3.55)$$

$$\begin{aligned} (3, 4) \text{ Basis: } & \{(3, 2, 3, 4), (3, 4, 3, 4), (3, 6, 3, 4), (3, 4, 5, 4)\} \\ \hat{\mathbf{U}}^{(4)4}(3, 4) &= \frac{\sqrt{3}-1}{2} \left(e^{-\frac{\lambda}{2}i}, -e^{\frac{11\lambda}{2}i}, -(\sqrt{3}+1)^{1/2} e^{-\frac{7\lambda}{2}i}, (\sqrt{3}+1)^{1/2} e^{\frac{11\lambda}{2}i} \right) \\ \hat{\mathbf{U}}^{(4)6}(3, 4) &= \frac{\sqrt{3}-1}{2} \left(-(\sqrt{3}+1)^{1/2} e^{-\frac{11\lambda}{2}i}, -(\sqrt{3}-1)^{1/2} e^{\frac{7\lambda}{2}i}, \sqrt{2} e^{-\frac{7\lambda}{2}i}, \sqrt{2} e^{\frac{7\lambda}{2}i} \right) \end{aligned} \quad (3.56)$$

$$\begin{aligned} (4, 3) \text{ Basis: } & \{(4, 3, 2, 3), (4, 3, 4, 3), (4, 5, 4, 3), (4, 3, 6, 3)\} \\ \hat{\mathbf{U}}^{(4)4}(4, 3) &= \frac{\sqrt{3}-1}{2} \left(e^{\frac{5\lambda}{2}i}, -e^{-\frac{7\lambda}{2}i}, (\sqrt{3}+1)^{1/2} e^{-\frac{7\lambda}{2}i}, -(\sqrt{3}+1)^{1/2} e^{\frac{11\lambda}{2}i} \right) \\ \hat{\mathbf{U}}^{(4)6}(4, 3) &= \frac{\sqrt{3}-1}{2} \left(-(\sqrt{3}+1)^{1/2} e^{\frac{11\lambda}{2}i}, -(\sqrt{3}-1)^{1/2} e^{-\frac{7\lambda}{2}i}, \sqrt{2} e^{-\frac{7\lambda}{2}i}, \sqrt{2} e^{\frac{7\lambda}{2}i} \right) \end{aligned} \quad (3.57)$$

For $n_5 = \hat{N}_3 + \hat{N}_5$:

$$(2,4) \text{ Basis: } \{(2,1,2,3,4), (2,3,2,3,4), (2,3,4,3,4), (2,3,4,5,4), (2,3,6,3,4)\}$$

$$\hat{U}^{(5)5}(2,4) = \frac{\sqrt{3}-1}{2} (-\sqrt{2}e^{3\lambda i}, (\sqrt{3}-1)^{1/2}e^{3\lambda i}, (\sqrt{3}-1)^{1/2}e^{-3\lambda i}, -\sqrt{2}e^{-3\lambda i}, -\sqrt{2})$$

$$\hat{U}^{(5)3}(2,4) = \left(\frac{2}{\sqrt{3}} - 1 \right)^{1/2} (-\sqrt{2}e^{3\lambda i}, (\sqrt{3}-1)^{1/2}e^{3\lambda i}, -(\sqrt{3}-1)^{1/2}e^{-\lambda i}, \sqrt{2}e^{-\lambda i}, e^{-5\lambda i}) \quad (3.58)$$

$$(3,3) \text{ Basis: } \{(3,2,1,2,3), (3,2,3,2,3), (3,2,3,4,3), (3,2,3,6,3), (3,4,3,2,3), (3,4,3,4,3)$$

$$(3,4,3,6,3), (3,6,3,2,3), (3,6,3,4,3), (3,6,3,6,3), (3,4,5,4,3)\}$$

$$\hat{U}^{(5)5}(3,3) = \left(\frac{\sqrt{3}-1}{2} \right)^{3/2} ((\sqrt{3}+1)^{1/2}, -1, i, (\sqrt{3}+1)^{1/2}e^{-3\lambda i}, -i, 1, -(\sqrt{3}+1)^{1/2}e^{-3\lambda i},$$

$$(\sqrt{3}+1)^{1/2}e^{3\lambda i}, -(\sqrt{3}+1)^{1/2}e^{3\lambda i}, 0, -(\sqrt{3}+1)^{1/2})$$

$$\hat{U}_1^{(5)3}(3,3) = \frac{1}{2}(1 - \frac{1}{\sqrt{3}})^{1/2} ((\sqrt{3}+1)^{1/2}e^{-2\lambda i}, -e^{-2\lambda i}, e^{-2\lambda i}, 0, e^{-2\lambda i}, -e^{-2\lambda i}, 0, 0, 0,$$

$$0, (\sqrt{3}+1)^{1/2}e^{-2\lambda i})$$

$$\hat{U}_2^{(5)3}(3,3) = 3^{-\frac{1}{4}} \left(\frac{\sqrt{3}-1}{2} \right)^{3/2} ((\sqrt{3}+1)^{1/2}e^{-5\lambda i}, -e^{-5\lambda i}, -\sqrt{3}e^{\lambda i}, (2(\sqrt{3}+1))^{1/2}e^{-\lambda i},$$

$$\sqrt{3}e^{\lambda i}, e^{-5\lambda i}, -(2(\sqrt{3}+1))^{1/2}e^{-\lambda i}, -(2(\sqrt{3}+1))^{1/2}e^{3\lambda i},$$

$$(2(\sqrt{3}+1))^{1/2}e^{3\lambda i}, 0, -(\sqrt{3}+1)^{1/2}e^{-5\lambda i}) \quad (3.59)$$

or any other orthonormal basis spanned by $\hat{U}_1^{(5)3}(3,3)$ and $\hat{U}_2^{(5)3}(3,3)$.

$$(4,2) \text{ Basis: } \{(4,3,2,1,2), (4,3,2,3,2), (4,3,4,3,2), (4,5,4,3,2), (4,3,6,3,2)\}$$

$$\hat{U}^{(5)5}(4,2) = \frac{\sqrt{3}-1}{2} (-\sqrt{2}e^{-3\lambda i}, (\sqrt{3}-1)^{1/2}e^{-3\lambda i}, (\sqrt{3}-1)^{1/2}e^{3\lambda i}, -\sqrt{2}e^{3\lambda i}, -\sqrt{2})$$

$$\hat{U}^{(5)3}(4,2) = \left(\frac{2}{\sqrt{3}} - 1 \right)^{1/2} (\sqrt{2}e^{-\lambda i}, -(\sqrt{3}-1)^{1/2}e^{-\lambda i}, (\sqrt{3}-1)^{1/2}e^{3\lambda i}, -\sqrt{2}e^{3\lambda i}, e^{-5\lambda i}) \quad (3.60)$$

The a -type seam weights, associated with the \hat{N}_a fusion projectors, are given by

$$W_{(1,a,1)} \left(\begin{array}{ccc} e & \nu & d \\ b & \mu & c \end{array} \right) = \begin{array}{c} e \quad \nu \quad d \\ \boxed{(1,a)} \\ b \quad \mu \quad c \end{array} = \lim_{u \rightarrow i\infty} \frac{e^{-i\frac{(g+1)(s-1)}{2}\lambda}}{s(u+\xi) s_{-1}^{s-2}(u+\xi)} \begin{array}{c} \hat{\mathbf{U}}_{\nu}^{(s)a} \big|_{(e,d)}^{\dagger} \\ \boxed{X^{(s-1)1}(u+\xi)} \\ \hat{\mathbf{U}}_{\mu}^{(s)a} \big|_{(b,c)} \end{array} \quad (3.61)$$

where s is chosen so that the corresponding fused adjacency matrix contains \hat{N}_a (2.11). Note that the choice of s to obtain a particular a -type seam is not unique. In the E_6 case, for example, we can obtain the \hat{N}_4 seam from $n_4 = \hat{N}_4 + \hat{N}_6$ or from $n_6 = \hat{N}_2 + \hat{N}_4$. Remarkably, the weights for such cases agree up to a unitary similarity transformation and give the same spectra for the transfer matrices.

As an example we give the a -type seam weights explicitly for E_6 :

$$\hat{N}_4 : \quad \begin{array}{c} 1 \quad 4 \\ \boxed{2} \quad 3 \end{array} = \begin{array}{c} 2 \quad 3 \\ 3 \quad 2 \end{array} = \begin{array}{c} 6 \quad 3 \\ 3 \quad 4 \end{array} = \begin{array}{c} 5 \quad 2 \\ 4 \quad 3 \end{array} = 1, \quad (3.62)$$

$$\begin{array}{c} 3 \quad 4 \\ 2 \quad 5 \end{array} = \begin{array}{c} 2 \quad 3 \\ 3 \quad 6 \end{array} = e^{-2i\lambda}, \quad \begin{array}{c} 1 \quad 4 \\ 2 \quad 5 \end{array} = \begin{array}{c} 5 \quad 2 \\ 4 \quad 1 \end{array} = e^{-\frac{9}{2}i\lambda} \quad (3.63)$$

$$\begin{array}{c} 6 \quad 3 \\ 3 \quad 2 \end{array} = e^{-i\frac{\lambda}{2}}, \quad \begin{array}{c} 4 \quad 3 \\ 3 \quad 4 \end{array} = -e^{i\frac{\lambda}{2}}, \quad \begin{array}{c} 6 \quad 3 \\ 3 \quad 6 \end{array} = -e^{-\frac{9}{2}i\lambda}, \quad \begin{array}{c} 3 \quad 2 \\ 4 \quad 1 \end{array} = -e^{-\frac{3}{2}i\lambda} \quad (3.64)$$

$$\begin{array}{c} 3 \quad 2 \\ 4 \quad 3 \end{array} = \frac{-1+\sqrt{3}}{2} e^{3i\lambda}, \quad \begin{array}{c} 3 \quad 4 \\ 2 \quad 3 \end{array} = \frac{1-\sqrt{3}}{2} e^{\frac{5}{2}i\lambda} \quad (3.65)$$

$$\hat{N}_6 : \quad \begin{array}{c} 2 \\ \square \\ 1 \end{array}^3 = \begin{array}{c} 2 \\ \square \\ 3 \end{array} = \begin{array}{c} 6 \\ \square \\ 3 \end{array}^5 = \begin{array}{c} 5 \\ \square \\ 4 \end{array}^6 = 1, \quad (3.66)$$

$$\begin{array}{c} 2 \\ \square \\ 3 \end{array} = -e^{\frac{9}{2}i\lambda}, \quad \begin{array}{c} 4 \\ \square \\ 3 \end{array} = -e^{-\frac{3}{2}i\lambda}, \quad \begin{array}{c} 6 \\ \square \\ 2 \end{array}^1 = -e^{\frac{3}{2}i\lambda}, \quad \begin{array}{c} 4 \\ \square \\ 2 \end{array}^3 = i \quad (3.67)$$

$$\hat{N}_5 : \quad \begin{array}{c} 2 \\ \square \\ 1 \end{array}^4 = \begin{array}{c} 4 \\ \square \\ 5 \end{array}^2 = \begin{array}{c} 6 \\ \square \\ 3 \end{array}^6 = 1, \quad \begin{array}{c} 2 \\ \square \\ 3 \end{array} = \begin{array}{c} 3 \\ \square \\ 4 \end{array}^3 = -i \quad (3.68)$$

Note that we can make the weights of the \hat{N}_5 and \hat{N}_6 seams real by changing the phase of the fusion vectors. Consequently, the corresponding partition functions are ambichiral since the transfer matrices contain only real entries and thus their eigenvalues must occur in complex conjugate pairs. Note also that the weights of the \hat{N}_5 seam can be transformed to be either 1 or 0. Thus the \hat{N}_5 seam is seen to be identical to the automorphism seam (3.31) which implements the \mathbf{Z}_2 involution on the E_6 graph.

For $D_{2\ell}$ cases, the ordinary fusion projectors are decomposed according to

$$n_s = \hat{N}_s, \quad 1 \leq s \leq 2\ell - 2, \quad \text{and} \quad n_{2\ell-1} = \hat{N}_{2\ell-1} + \hat{N}_{2\ell} \quad (3.69)$$

and the a -type seams for $\hat{N}_{2\ell-1}$ and $\hat{N}_{2\ell}$ can be obtained by the same process applied to E_6 . In the D_4 case, the \hat{N}_3 and \hat{N}_4 a -type seams

$$\hat{N}_3 : \quad \begin{array}{c} 1 \\ \square \\ 2 \end{array}^3 = 1, \quad \begin{array}{c} 4 \\ \square \\ 2 \end{array}^1 = \begin{array}{c} 2 \\ \square \\ 3 \end{array}^2 = e^{2\pi i/3} \quad (3.70)$$

$$\hat{N}_4 : \quad \begin{array}{c} 1 \\ \square \\ 2 \end{array}^4 = 1, \quad \begin{array}{c} 3 \\ \square \\ 2 \end{array}^1 = \begin{array}{c} 2 \\ \square \\ 4 \end{array}^2 = e^{2\pi i/3} \quad (3.71)$$

are identical, up to the phase of the fusion vectors, to the \mathbf{Z}_3 automorphism seams and yield ambichiral partition functions.

3.6 Construction of a -type seams for Type II theories

So far we have discussed only the a -type seam of Type I graphs. On a Type II graph G , the seam cannot be associated with \hat{N}_a since these graph fusion matrices contain negative integers which fail to give a meaningful description in terms of lattice paths. Instead, for a Type II graph, an a -type seam must be associated with a node $a \in H$ in the parent Type I graph rather than to a node $a \in G$. For the A - D - E graphs, only $D_{2\ell+1}$ and E_7 are of Type II. For $D_{2\ell+1}$ we do not need a -type seams only the r - and s -type seams. So here we consider only the case of $G = E_7$ with parent graph $H = D_{10}$.

The s -type seams of E_7 constructed via (3.28) are labelled by $s \in A_{17}$. We decompose these according to (3.69)

$$n_s = n_s^{(E_7 D_{10})}, \quad 1 \leq s \leq 8, \quad \text{and} \quad n_9 = n_9^{(E_7 D_{10})} + n_{10}^{(E_7 D_{10})} \quad (3.72)$$

where the intertwiners $\{n_a^{(E_7 D_{10})}\}_{a \in D_{10}}$ of E_7 relative to D_{10} (3.25) form a representation of

the D_{10} graph fusion algebra. Explicitly, we have

$$n_9 = \begin{pmatrix} 1 & 0 & 1 & 0 & 0 & 0 & 1 \\ 0 & 2 & 0 & 2 & 0 & 0 & 0 \\ 1 & 0 & 3 & 0 & 2 & 0 & 1 \\ 0 & 2 & 0 & 4 & 0 & 2 & 0 \\ 0 & 0 & 2 & 0 & 2 & 0 & 2 \\ 0 & 0 & 0 & 2 & 0 & 0 & 0 \\ 1 & 0 & 1 & 0 & 2 & 0 & 1 \end{pmatrix} = \begin{pmatrix} 0 & 0 & 1 & 0 & 0 & 0 & 0 \\ 0 & 1 & 0 & 1 & 0 & 0 & 0 \\ 0 & 0 & 1 & 0 & 1 & 0 & 1 \\ 0 & 1 & 0 & 2 & 0 & 1 & 0 \\ 0 & 0 & 1 & 0 & 1 & 0 & 1 \\ 0 & 0 & 0 & 1 & 0 & 0 & 0 \\ 0 & 0 & 1 & 0 & 1 & 0 & 0 \end{pmatrix} + \begin{pmatrix} 1 & 0 & 0 & 0 & 0 & 0 & 1 \\ 0 & 1 & 0 & 1 & 0 & 0 & 0 \\ 0 & 0 & 2 & 0 & 1 & 0 & 0 \\ 0 & 1 & 0 & 2 & 0 & 1 & 0 \\ 0 & 0 & 1 & 0 & 1 & 0 & 1 \\ 0 & 0 & 0 & 1 & 0 & 0 & 0 \\ 1 & 0 & 0 & 0 & 1 & 0 & 1 \end{pmatrix} \\ = n_9^{(E_7 D_{10})} + n_{10}^{(E_7 D_{10})} \quad (3.73)$$

The $n_a^{(E_7 D_{10})}$ fusion vectors for E_7 can be obtained by unitary transformation. However, as n_9 is complicated, we need to introduce another unitary transformation formula before we proceed. Since (3.45) is unitary, its inverse is also unitary. By the same argument, suppose that $\hat{U}_\mu^{(s)a}(e, d)$ is known for some given s, d, e . Then for any $b, c \in G$ with $\hat{N}_{ab}^c \neq 0$ satisfying

$$n_{2e}^b \neq 0 \quad \text{and} \quad n_{sb}^{c'} n_{2c'}^d = n_{sb}^c \delta_{c',c} \quad (3.74)$$

the \hat{N}_a fusion vector $\hat{U}_\mu^{(s)a}(b, c)$ is given by the unitary transformation

$$\hat{U}_\mu^{(s)a}(e, d) \mapsto \hat{U}_\mu^{(s)a}(b, c) : \quad \hat{U}_\mu^{(s)a}(b, c) = \begin{array}{c} \text{Diagram showing a rectangle with vertices } b, c, d, e. \text{ The top edge is labeled } X^{(s-1)1}, \text{ the right edge } (+i\infty), \text{ and the bottom edge } \hat{U}_\mu^{(s)a}(e, d). \end{array} \quad (3.75)$$

and can be expressed as

$$\hat{U}_\mu^{(s)a}(b, c) = \sum_{\gamma} W_{(1,s,1)} \begin{pmatrix} b & \gamma & c \\ e & \mu & d \end{pmatrix} U_{\gamma}^s(b, c) \quad (3.76)$$

Comparing (3.76) with (3.47) we note that it does not contain the crossing factor. Depending on the condition (3.44) or (3.74), the unknown \hat{N}_a fusion vectors can be obtained from known ones by either (3.47) or (3.76).

Note, however, that for $(b, c) = (3, 3)$ in n_9 , there does not exist (e, d) which satisfy either (3.44) or (3.74). Thus, we need to extend the range of the transformation in order to make it unitary

$$\begin{aligned} \{\hat{U}^{(9)10}(2, 2), \hat{U}^{(9)10}(2, 4)\} &\xrightarrow{(3.47)} \{\hat{U}_1^{(9)10}(3, 3), \hat{U}_2^{(9)10}(3, 3)\} \\ \{\hat{U}^{(9)9}(2, 2), \hat{U}^{(9)9}(2, 4)\} &\xrightarrow{(3.47)} \{\hat{U}^{(9)9}(3, 3), U(1, 3)\} \end{aligned} \quad (3.77)$$

and the transformations to $\hat{U}_\mu^{(9)a}(3, 3)$ for both $a = 9, 10$ must be in the nullspace of $U(1, 3)$. Thus

$$\hat{U}^{(9)9}(3, 3) = \sqrt{\frac{\psi_1 \psi_4}{\psi_3(\psi_2 + \psi_4)}} \left(\sqrt{\frac{\psi_2 \psi_3}{\psi_2 \psi_1}} \begin{array}{c} \text{Diagram showing a rectangle with vertices } 2, 3, 3, 2. \text{ The top edge is labeled } X^{18}, \text{ the right edge } (-i\infty), \text{ and the bottom edge } \hat{U}^{(9)9}(2, 2). \end{array} - \sqrt{\frac{\psi_2 \psi_3}{\psi_4 \psi_1}} \begin{array}{c} \text{Diagram showing a rectangle with vertices } 2, 3, 3, 4. \text{ The top edge is labeled } X^{18}, \text{ the right edge } (-i\infty), \text{ and the bottom edge } \hat{U}^{(9)9}(2, 4). \end{array} \right) \quad (3.78)$$

where the scalar factors in (3.78) cancel the crossing factors in (3.47) when we take the inverse of $\mathbf{U}(1,3) \mapsto \hat{\mathbf{U}}^{(9)9}(2,2)$ and $\mathbf{U}(1,3) \mapsto \hat{\mathbf{U}}^{(9)9}(2,4)$ respectively.

There are 58 possible spin configurations for non-zero s -type seam weights $W_{(1,9,1)}^1$. We constructed all the a -type seams for $n_9^{(E_7 D_{10})}$ and $n_{10}^{(E_7 D_{10})}$ symbolically and confirmed that (3.41) is satisfied for all possible spin configurations at the four corners of the seam weight and for all possible bond variables. Note that, by the quantum symmetry, the partition functions of $x = (a,b) = (9,1)$ and $(3,1)$ are complex conjugates. Thus, the spectra of the transfer matrices of the respective $n_9^{(E_7 D_{10})}$ and n_3 seams must be complex conjugates and this is verified numerically.

4 Transfer Matrices

Given the fusion hierarchy, we build commuting transfer matrices for different fusion levels and boundary conditions: on the torus and on the cylinder, with or without seams.

4.1 Torus transfer matrices

The transfer matrix for the (p,q) -fused A - D - E lattice model with an (r,s,η) -seam, on a toroidal square lattice is given, in the basis of the cyclic paths in N steps plus the seam, with bond variables between adjacent spins, by the product of the corresponding Boltzmann weights. The entries of the transfer matrix with an (r,s,η) seam are given by

$$\langle \mathbf{a}, \boldsymbol{\alpha} | \mathbf{T}_{(r,s,\eta)}^{pq}(u, \xi) | \mathbf{b}, \boldsymbol{\beta} \rangle = \begin{array}{c} b_1 & \beta_1 & b_2 & & b_N & \beta_N & b_{N+1} & \beta_{N+1} & b_{N+2} & \beta_{N+2} & b_{N+3} & b_1 \\ \hline u & & & \cdots & u & & u & & r(u, \xi) & & (1,s) & \eta \\ \hline a_1 & \alpha_1 & a_2 & & a_N & \alpha_N & a_{N+1} & \alpha_{N+1} & a_{N+2} & \alpha_{N+2} & a_{N+3} & a_1 \end{array} = \sum_{\gamma} \prod_{i=1}^N W^{pq} \left(\begin{array}{ccc|c} b_i & \beta_i & b_{i+1} & u \\ \gamma_i & & \gamma_{i+1} & \\ a_i & \alpha_i & a_{i+1} & \end{array} \right) W_{(r,1)}^q \left(\begin{array}{ccc|c} b_N & \beta_N & b_{N+1} & u, \xi \\ \gamma_N & & \gamma_{N+1} & \\ a_N & \alpha_N & a_{N+1} & \end{array} \right) \times W_{(1,s)}^q \left(\begin{array}{ccc} b_{N+1} & \beta_{N+1} & b_{N+2} \\ \gamma_{N+1} & & \gamma_{N+2} \\ a_{N+1} & \alpha_{N+1} & a_{N+2} \end{array} \right) W_{(1,1,\eta)}^q \left(\begin{array}{cc} b_{N+2} & b_1 \\ \gamma_{N+2} & \gamma_1 \\ a_{N+2} & a_1 \end{array} \right) \quad (4.1)$$

where the sum is over all allowed vertical bond variables. The usual periodic boundary condition is obtained for $(r,s,\eta) = (1,1,1)$. The s -type seam can be replaced with a single a -type seam or a pair of a and b seams. Recall that the a and b -type seams derive from the two braid limits $u \rightarrow \pm i\infty$ respectively of the s -type seams and are related by complex conjugation. Indeed the definition can be generalized to accommodate an arbitrary number of seams. Because the seam faces, other than the automorphism seams, are modified bulk faces they automatically satisfy the GYBE. They can therefore be moved around freely with respect to each other and the bulk faces without effecting the spectrum of the transfer matrices. However, in the $D_{2\ell}$ cases when there are several seams, their order in general

cannot be interchanged because the automorphism seams do not commute with the a -type seams.

4.2 Non-commutativity of seams

To understand the origin of non-commutativity of seams let us begin by considering D_4 . The graph D_4 exhibits an \mathbf{S}_3 symmetry on the external nodes $T = \{1, 3, 4\}$. This permutation group contains non-commuting two- and three-cycles

$$\mathbf{S}_3 = \{(); (1\ 3), (1\ 4), (3\ 4); (1\ 3\ 4), (1\ 4\ 3)\} \quad (4.2)$$

In the lattice model seams, these symmetries are realized by the \mathbf{Z}_2 and \mathbf{Z}_3 automorphism seams (3.31) with $\eta \in \mathbf{S}_3$. Notice however that the graph fusion matrix \hat{N}_3 implements the permutation $(1\ 3\ 4)$ and \hat{N}_4 implements the permutation $(1\ 4\ 3)$. Accordingly, on the lattice these automorphisms are implemented by the a -type seams with $a = 3, 4$. This means that the fused seams need only be supplemented by the \mathbf{Z}_2 transposition $\sigma = (3\ 4)$ to generate all of \mathbf{S}_3 . Moreover, D_4 is the only graph with an automorphism group other than \mathbf{Z}_2 , so we can always restrict to automorphisms $\eta = \sigma^{\kappa-1} \in \mathbf{Z}_2$, $\kappa = 1, 2$.

The fused seams, together with the bulk face weights, satisfy the generalized Yang-Baxter equation and thus they commute with each other and can propagate through the bulk face weights along the row [4]. Two transfer matrices differing by a propagation of fused seams differ only by a similarity transformation. Thus the spectrum of the torus transfer matrices with a given set of regular fused seams does not depend on the order of these seams nor on their positions. On the other hand, the automorphism seams commute with the bulk face weights and the r - and s -type fused seams but not, in general, with the a -type seams related to \hat{N} fusions. This is manifest in the D_4 case since the transposition $(3\ 4)$ does not commute with the three-cycles $(1\ 3\ 4)$ and $(1\ 4\ 3)$ implemented by \hat{N}_3 and \hat{N}_4 .

Consider several such seams on the lattice. The non-commutativity of seams shows up by the fact that we get different resultant seams when placing given seams in different order. For instance, if $\sigma = (3\ 4)$

$$(1\ 4\ 3)(3\ 4)(1\ 3\ 4)(3\ 4) = (1\ 3\ 4), \quad (1\ 4\ 3)(1\ 3\ 4)(3\ 4)(3\ 4) = () \quad (4.3)$$

and accordingly the product of four (r, a, η) seams

$$W_{(1,4,1)}W_{(1,1,\sigma)}W_{(1,3,1)}W_{(1,1,\sigma)} \sim W_{(1,3,1)} \quad (4.4)$$

gives the same spectrum as the single seam $W_{(1,3,1)}$ whereas the combination of seams

$$W_{(1,4,1)}W_{(1,3,1)}W_{(1,1,\sigma)}W_{(1,1,\sigma)} \sim W_{(1,1,1)} \quad (4.5)$$

yields the modular invariant partition function. Notice that $W_{(1,3,1)}W_{(1,1,\sigma)} \sim W_{(1,1,\sigma)}W_{(1,3,1)}$ gives the same spectra even though $(1\ 3\ 4)(3\ 4) \neq (3\ 4)(1\ 3\ 4)$ since the positions of the two seams can be interchanged by propagating one of them full cycle around the periodic row. Consequently, four or more seams are required to see the effects of non-commutativity in the spectra.

The same phenomenon is exhibited for the whole family $D_{2\ell}$ of Type I models. The a -type seams $(1, 2\ell - 1, 1)$, $(1, 2\ell, 1)$ related to $\hat{N}_{2\ell-1}$ and $\hat{N}_{2\ell}$ do not commute with the automorphism seam $(1, 1, \sigma)$ where $\sigma = (2\ell - 1, 2\ell)$ is the \mathbf{Z}_2 transposition, although their sum does commute as indicated by the relation $\hat{N}_{2\ell-1}\sigma = \sigma\hat{N}_{2\ell}$.

4.3 Integrable seams on the cylinder

Although twisted partition functions occur on the torus, it is striking to see that the Ocneanu algebra still plays a role on the cylinder. Indeed, Petkova and Zuber [25] give the minimal conformal partition functions on the cylinder with a seam x and boundary conditions (r, a) and (r', b) as

$$Z_{(r,a)|x|(r',b)}(q) = \sum_{(r,s)} \delta_{r,r'} (n_s \tilde{n}_x)_a^b \chi_{r,s}(q) \quad (4.6)$$

Another remarkable observation [7] is that the twisted partition functions on the torus can be written as a bilinear combination of cylinder partition functions, summed over some boundary conditions.

In fact, the Ocneanu graph labelling the seams gives a complete set of boundary conditions, not only on the torus but also on the cylinder for the continuous conformal field theory as well as for the integrable statistical mechanics model. In the latter context, a full set of integrable boundary weights of type (r, a) for Type I theories can be obtained by propagating a seam of type (r, a) to the boundary and combining it with the simplest boundary condition $(r, a) = (1, 1)$ called the vacuum. Similarly, for Type II theories, the seams (r, c) with c in the parent graph H can be propagated to the boundary to produce an integrable boundary condition by combining it with the vacuum. However, in this case, only $|G|$ of the $|H|$ values for c produce linearly independent boundary conditions. This is in accord with the fact that only $|G|$ of the $|H|$ intertwiners $n_c^{(G H)}$ of G relative to H are linearly independent

$$n_c^{(G H)} = \sum_{a \in G} \tilde{n}_{ca}^{-1} \hat{N}_a^{(G)} \quad (4.7)$$

In other words, although G -type boundary conditions are applied on the edge of the cylinder, only H -type seams propagate into the bulk. With this caveat, the algebra of defect lines (or seams) can be applied on the cylinder as well.

The vacuum boundary condition corresponds to $(r, a) = (1, 1)$. The $(1, a)$ boundary weights, for two q -adjacent nodes of G , c and a (i.e. $n_{q+1,a}^c \neq 0$) are given by

$$B_{(1,a)}^q \begin{pmatrix} \gamma & a \\ c & \alpha \\ & a \end{pmatrix} = c \begin{array}{c} \nearrow \gamma \\ \searrow (1,a) \\ \alpha \end{array} = \frac{\psi_c^{1/2}}{\psi_a^{1/2}} \mathbf{U}_\gamma^{q+1}(c, a)^\dagger \mathbf{U}_\alpha^{q+1}(c, a) = \frac{\psi_c^{1/2}}{\psi_a^{1/2}} \delta_{\gamma\alpha} . \quad (4.8)$$

In the Type I case, it is obtained by the action of an a -seam on the vacuum boundary condition. The full (r, a) boundary weights are then given by the action of an r -type seam on the $(1, a)$ -boundary weight. The double row seams are given by two regular r -seams sharing the same extra spectral parameter ξ , placed one on top of the other, with the same

spectral parameters as the bulk faces appearing in the double row transfer matrix (see (4.11))

$$B_{(r,a)}^q \begin{pmatrix} d & \delta \\ c & \alpha \\ b & \beta \end{pmatrix} \Big| u, \xi = c \begin{array}{c} d \\ \diagup (r,a) \\ \diagdown (u,\xi) \\ \alpha \\ \beta \end{array} = c \begin{array}{c} d \\ \delta \\ \diagup r(\mu-u-(q-1)\lambda, \xi) \\ \alpha \\ \beta \end{array} \dots a \quad (4.9)$$

and the left boundary weights are simply equal to the right boundary weights after applying crossing symmetry.

These boundary weights satisfy boundary analogs of the bulk local relations. The Generalized Boundary Yang-Baxter Equation or reflection equation is

$$\begin{array}{c} b \\ \diagup \beta \\ \diagdown u-p \\ \diagup \mu-u-v \\ \diagdown (q-1)\lambda \\ \diagup \delta \\ \diagdown d \\ \diagup e \\ \diagdown f \end{array} = \frac{s_{1+q-p}^{qp}(u-v) s_{1-(p-1)}^{qp}(\mu-u-v)}{s_1^{pq}(u-v) s_{1-(q-1)}^{pq}(\mu-u-v)} \begin{array}{c} b \\ \diagup \beta \\ \diagdown u-v \\ \diagup \mu-(q-1)\lambda \\ \diagdown \delta \\ \diagup e \\ \diagdown f \end{array} \quad (4.10)$$

which is proved using the GYBE (3.16) and the abelian property (3.3). We refer to [4, 24] for the boundary crossing equation.

The double row transfer matrix is given by two rows similar to the one appearing in the torus transfer matrix, with spectral parameters u for the bottom one and $\mu - u - (q-1)\lambda$ for the top one, where μ is a fixed parameter and q is the vertical fusion level. The boundary condition is not cyclic but given by the boundary weights (4.9).

$$\langle \mathbf{a}, \boldsymbol{\alpha} | \mathbf{T}_{(r_L, a_L) | (r, s, \eta) | (r_R, a_R)}^{pq}(u, \xi_L, \xi, \xi_R) | \mathbf{b}, \boldsymbol{\beta} \rangle =$$

$$\begin{array}{cccccccccc} a_L & & b_1 & & b_2 & & b_N & & b_{N+1} & & b_{N+2} & & b_{N+3} & & b_{N+4} & & a_R \\ \beta_L & \dots & \beta_1 & & \beta_2 & & \beta_N & & \beta_{N+1} & & \beta_{N+2} & & \beta_{N+3} & & \beta_{N+4} & & \beta_R \\ \diagup (r_L, a_L) & & \big(\mu-u-(q-1)\lambda \big) & & & & \big(\mu-u-(q-1)\lambda \big) & & \big(\mu-u-(q-1)\lambda, \xi \big) & & (1, s) & & \eta & & & & \diagup (r_R, a_R) \\ \diagdown (\mu-u, \xi_L) & & \diagdown \alpha_L & & \diagdown \alpha_1 & & \diagdown \alpha_2 & & \diagdown \alpha_N & & \diagdown \alpha_{N+1} & & \diagdown \alpha_{N+2} & & \diagdown \alpha_{N+3} & & \diagdown \alpha_R & & \diagdown a_R \end{array} \quad (4.11)$$

The GYBE (3.16) and other local relations imply that double row transfer matrices with the same boundary conditions and boundary fields commute

$$\begin{aligned} & \mathbf{T}_{(r_L, a_L) | (r, s, \eta) | (r_R, a_R)}^{pq}(u, \xi_L, \xi, \xi_R) \mathbf{T}_{(r_L, a_L) | (r, s, \eta) | (r_R, a_R)}^{pq'}(v, \xi_L, \xi, \xi_R) = \\ & \mathbf{T}_{(r_L, a_L) | (r, s, \eta) | (r_R, a_R)}^{pq'}(v, \xi_L, \xi, \xi_R) \mathbf{T}_{(r_L, a_L) | (r, s, \eta) | (r_R, a_R)}^{pq}(u, \xi_L, \xi, \xi_R). \end{aligned} \quad (4.12)$$

5 Finite-Size Corrections and Numerical Spectra

5.1 Finite-size corrections and conformal spectra

A critical A - D - E lattice model with a spectral parameter in the range $0 < u < \lambda$ gives rise to a conformal field theory in the continuum scaling limit, namely, an $\hat{sl}(2)$ unitary minimal model. The properties of the A - D - E lattice model connect to the data of this conformal field theory through the finite-size corrections to the eigenvalues of the transfer matrices.

Consider a periodic row transfer matrix $\mathbf{T}(u, \xi)$ with a seam x of type (r, s, η) or (r, a, η) and N faces excluding the seams. If we write the eigenvalues of this transfer matrix as

$$T_n(u) = \exp(-E_n(u)), \quad n = 0, 1, 2, \dots \quad (5.1)$$

then the finite-size corrections to the energies E_n take the form

$$E_n(u) = Nf(u) + f_r(u, \xi) + \frac{2\pi}{N} \left(\left(-\frac{c}{12} + \Delta_n + \bar{\Delta}_n + k_n + \bar{k}_n \right) \sin \vartheta + i(\Delta_n - \bar{\Delta}_n + k_n - \bar{k}_n) \cos \vartheta \right) + o\left(\frac{1}{N}\right) \quad (5.2)$$

where $f(u)$ is the bulk free energy, $f_r(u, \xi)$ is the boundary free energy (independent of s , a and η), c is the central charge, Δ_n and $\bar{\Delta}_n$ are the conformal weights, $k_n, \bar{k}_n \in \mathbf{N}$ label descendent levels and the anisotropy angle ϑ is given by

$$\vartheta = gu \quad (5.3)$$

where g is the Coxeter number.

On a finite $M \times N$ periodic lattice, the partition function can be written as

$$\begin{aligned} Z_x^{M,N} &= \exp(-MNf(u) - Mf_r(u, \xi)) Z_x(q) \\ &= \text{Tr } \mathbf{T}(u, \xi)^M = \sum_n T_n(u)^M = \sum_{n \geq 0} \exp(-ME_n(u)) \end{aligned} \quad (5.4)$$

where $Z_x(q)$ is the conformal partition function and $q = \exp(2\pi i\tau)$ is the modular parameter with $\tau = \frac{M}{N} \exp[i(\pi - \vartheta)]$. Removing the bulk and boundary contributions to the partition function on a torus leads to the twisted partition functions $Z_x(q)$ [7] described in Sections 2.3 and 2.4.

5.2 Bulk and seam free energies

In [26], we showed that the row transfer matrix with an (r, s, η) -seam satisfies the inversion identity hierarchy

$$\mathbf{T}_0^1 \mathbf{T}_1^1 = s_{-1}^{r-1} s_1^{r-1} f_{-1}^1 f_1^1 \mathbf{I} + s_0^{r-1} f_0^1 \mathbf{T}_0^2 \quad (5.5)$$

where $\mathbf{T}_k^q = \mathbf{T}_{r,s}^q(u + k\lambda)$ are vertically q -fused transfer matrices,

$$f_q^p = [s_q^p(u)]^N, \quad s_q^p = \begin{cases} 1 & r = 1, \\ s_q^p(u + \xi) & r \geq 2 \end{cases} \quad (5.6)$$

In the thermodynamic limit, the second term in (5.5) vanishes and the resulting formula is called an *Inversion Relation*. This equation can be solved, using the structure of zeros and poles, first at order N and then at order 1 to find the bulk and seam free energies as we explain in this section.

We calculate the bulk and seam free energies, $f(u)$ and $f_r(u, \xi)$, or equivalently the partition function per face $\kappa(u) = \exp(-f(u))$ and partition function per length $\kappa_r(u, \xi) = \exp(-f_r(u, \xi))$. Two *A-D-E* models sharing the same Coxeter number are related by inter-twiners so their bulk and seam free energies are the same. Thus we only need to find the free energies for the A_L or ABF models [17].

The bulk free energy $f(u) = -\log \kappa(u)$ for the ABF models was computed by Baxter

$$\kappa(u) = \exp \int_{-\infty}^{+\infty} \frac{\cosh(\pi - 2\lambda)t \sinh ut \sinh(\lambda - u)t}{t \sinh \pi t \cosh \lambda t} dt. \quad (5.7)$$

This integral has a closed form when L is even

$$\kappa(u) = \frac{\sin(u + \lambda)}{\sin \lambda} \prod_{k=1}^{\frac{L-2}{2}} \frac{\sin(u + (2k+1)\lambda)}{\sin(u + 2k\lambda)}. \quad (5.8)$$

The partition function per face of the A_L model satisfies the *crossing symmetry*

$$\kappa(u) = \kappa(\lambda - u) \quad (5.9)$$

and the *inversion relation*

$$\kappa(u) \kappa(u + \lambda) = \frac{\sin(u + \lambda) \sin(u - \lambda)}{\sin^2 \lambda}. \quad (5.10)$$

This solution is the unique solution of the inversion relation, crossing symmetry and height reversal symmetry which is analytic and non-zero in the analyticity strip $\text{Re } u \in (0, \lambda)$.

Likewise, the seam inversion relation for the order one term gives

$$\kappa_r(u) \kappa_r(u + \lambda) = \frac{\sin(u + \xi + \lambda) \sin(u + \xi - (r-1)\lambda)}{\sin^2 \lambda}. \quad (5.11)$$

The range of validity for the parameter ξ is

$$-\lambda - \frac{\pi}{2} < \text{Re}(u + \xi) < -\frac{\lambda}{2} \quad (5.12)$$

Let q be the RHS of (5.11). It is Analytic and Non-Zero in the strip $\text{Re } u \in (0, \lambda)$. Furthermore the derivative q' approaches a Constant when $\text{Im } u \rightarrow \pm\infty$ (ANZC). Hence we can introduce the Fourier transforms of the logarithmic derivatives

$$\mathcal{F}(k) := \frac{1}{2\pi i} \int_{0 < \text{Re } u < \lambda} f'_r(u) e^{-ku} du \quad (5.13)$$

$$\frac{d}{du} f_r(u) = \int_{-\infty}^{+\infty} \mathcal{F}(k) e^{ku} dk \quad (5.14)$$

so that (5.11) becomes

$$\mathcal{F}(k)(1 + e^{k\lambda}) = \frac{1}{2i\pi} \int_{0 < \text{Re}(u) < \lambda} \frac{q'(u)}{q(u)} e^{-ku} du \quad (5.15)$$

The solution by inverse Fourier transforms gives

$$\frac{d}{du} f_r(u) = \frac{1}{2i\lambda} \int_{0 < \text{Re} w < \lambda} dw \left(\frac{d}{du} \log q(u-w) \right) \frac{1}{\sin(L+1)w} \quad (5.16)$$

Integrating with respect to u and taking the w integration along the vertical line $\text{Re } w = \epsilon > 0$ we obtain in the limit $\epsilon \rightarrow 0$

$$f_r(u) = \frac{\log q(u)}{2} + \frac{1}{\lambda} \int_{-\infty}^{\infty} \frac{\log q(u-iw)}{\sinh(L+1)w} dw \quad (5.17)$$

This integral formula admits a closed form under certain conditions

$$\kappa_r(u) = \begin{cases} \frac{(u+\xi)}{\tan \frac{L+1}{2}(u+\xi)} \prod_{k=1}^{\frac{r-1}{2}} \frac{(u+\xi-2k\lambda)}{(u+\xi-(2k-1)\lambda)}, & r \text{ odd} \\ \frac{(u+\xi+\lambda)}{\tan \frac{L+1}{2}(u+\xi+\lambda)} \prod_{k=1}^{\frac{L-r}{2}} \frac{(u+\xi+(2k+1)\lambda)}{(u+\xi+2k\lambda)}, & L+r \text{ even.} \end{cases} \quad (5.18)$$

The tangent parts are solutions of the homogeneous functional equation and fix up the zeros and poles of the sine parts which are solutions of the functional equation (5.11) but have an unwanted zero in the analyticity strip.

The seam free energy for s -type seams are given by the braid limit of the r -type seams and are constants. The seam free energies of the a -type seams are the same as the s -type seam from which they originate. We remove these seam free energies by the normalization of the transfer matrices. Lastly, the seam free energy of an η seam is zero.

5.3 Numerical determination of conformal spectra

The twisted conformal partition functions are obtained numerically from finite-size spectra. Since integrable lattice realizations of the $sl(2)$ A - D - E Wess-Zumino-Witten conformal field theories are not known we can only obtain numerically the twisted partition functions of the unitary minimal A - D - E models labelled by a pair of graphs (A, G) . We use Mathematica [27] to construct and diagonalize numerically the finite-size transfer matrices $\mathbf{T}(u, \xi)$ with specified seams for different numbers of faces N . For simplicity, we restrict ourselves to the isotropic conformal point given by $u = \frac{\lambda}{2}$ and $\xi = -3\lambda/2$. For the first ten or so eigenvalues, we extrapolate the conformal corrections to $N = \infty$ using a combination of polynomial fits in the inverse number of faces and van den Broeck-Schwartz [28] sequence extrapolation. The resulting sequences give approximations to the rational exponents that appear in the q -expansion of the twisted partition functions in increasing powers of the modular parameter q .

In subsequent subsections, we analyse the numerical data for the D_4, D_5, D_6 cases of the A - D - E lattice models. The A_L cases for $L = 3, 4, 5, 6, 7, 9$ were reported in [13]. All the numerical results confirm the quantum symmetries and twisted partition functions stated in Sections 2.3 and 2.4. Given the coincidence of the construction labels of our integrable seams and the conformal labels of Petkova and Zuber, we expect that our list of integrable seams will also exhaust the twisted conformal boundary conditions for the exceptional E_6, E_7 and E_8 cases as well. These cases, however, are too large to convincingly confirm numerically.

Consideration of a seam of type (r, a) gives access only to a chiral half of the Ocneanu graph. In general, to obtain the complete Ocneanu graph, one needs to consider the composition of two seams (r, a, η) and (r', b, η') . Since the A - D - E models are labelled by pairs (A, G) , with the first member always for type- A , it is sufficient to take $r' = r$. Also, as we have seen, we can restrict the automorphisms to a \mathbf{Z}_2 subgroup of the full automorphism group given by $\eta = \sigma^{\kappa-1}$. Indeed, the only graph G with an automorphism group larger than \mathbf{Z}_2 is D_4 and, in this case, the three-cycles of \mathbf{S}_3 are reproduced within the \hat{N} graph fusions. We conclude that it suffices to consider integrable seams of the form $x = (r, a, b, \sigma^{\kappa-1})$.

For simplicity, we take the absolute values of the eigenvalues which is equivalent to taking the modular parameter q real

$$|T_n^{(N)}| = e^{-Nf - f_r + \frac{2\pi}{N} \frac{c}{12}} \exp\left(-\frac{2\pi}{N} x_n + o\left(\frac{1}{N}\right)\right) \quad (5.19)$$

We thus numerically estimate the conformal dimensions or exponents

$$x_n = \Delta + \bar{\Delta} + k_n + \bar{k}_n \quad (5.20)$$

and ignore the spins $s_n = \Delta - \bar{\Delta} + k_n - \bar{k}_n$. Since we are at the isotropic point the geometric factor $\sin \vartheta = 1$. To obtain the bulk free energy, we extrapolate the sequence $-\frac{1}{N} \log |T_n^{(N)}|$. The seam free energy is obtained, in a similar way, after removing the bulk contribution in (5.19). An s - or a -type seam contributes a constant to the seam free energy which is removed by our choice of normalization. The extrapolated numerical values for the bulk and seam free energies agree with the analytic results (5.7) and (5.17) within an accuracy of $\pm 0.3\%$.

To estimate the exponents x_n , we extrapolate the sequences

$$x_n^{(N)} = -\frac{N}{2\pi} \left(\log |T_n^{(N)}| + Nf + f_r - \frac{2\pi}{N} \frac{c}{12} \right) \quad (5.21)$$

and compare values and degeneracies with q -series of the twisted partition functions $Z_x(q)$ [7].

The accuracy of our numerical results is restricted by the data for different system sizes N which, in turn, is limited by available computer memory. A typical maximum size matrix that we can construct and diagonalize is around 4500×4500 . The dimension of a transfer matrix with N faces and an (r, a) seam is $\text{Tr}(n_2^N n_r \hat{N}_a)$. This grows rapidly as the number of nodes in G increases and grows exponentially with N . In practice, this means we are typically restricted to $|G| \leq 6$ and to system sizes $N \leq 12$. Furthermore, because of parity constraints, we are either restricted to odd or even system sizes N so we

are typically extrapolating sequences of length six. Nevertheless, because of the quantized values of the conformal weights, the integer spacing of conformal towers and recognizable degeneracies of the characters, we are able to identify the various twisted partition functions with considerable confidence.

5.4 Numerical spectra of (A_4, D_4)

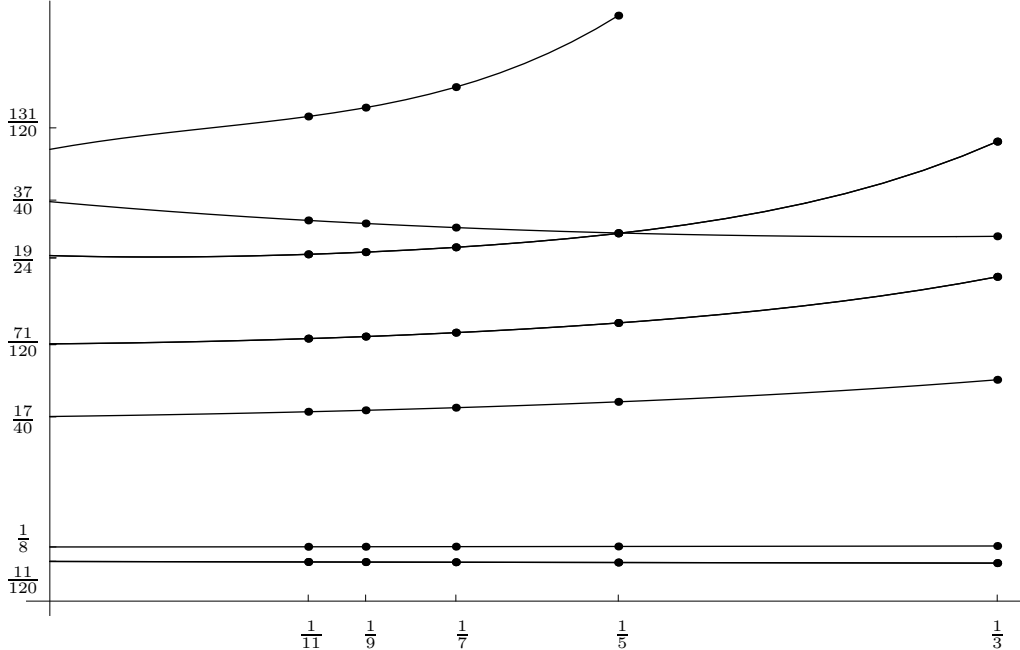


Figure 6: Energy levels of the minimal (A_4, D_4) model with $(1, 2, 1)$ seam. The numerical values of $x_n^{(N)}$ are plotted against $1/N$. The polynomial fits intersect the y -axis at the extrapolated values x_n . Notice that eigenvalues can cross for small values of N .

The (A_4, D_4) lattice model corresponds to the critical 3-state Potts model and is special in that the D_4 graph admits an S_3 automorphism group. However, we only need seams of the form $(r, a, \kappa) \equiv (r, a, \sigma^{\kappa-1})$ with $\kappa = 1, 2$ and $\sigma = (3\ 4)$ the \mathbf{Z}_2 transposition represented by

$$\sigma = \begin{pmatrix} 1 & 0 & 0 & 0 \\ 0 & 1 & 0 & 0 \\ 0 & 0 & 0 & 1 \\ 0 & 0 & 1 & 0 \end{pmatrix} \quad (5.22)$$

To illustrate our numerical procedure consider the twisted partition function $Z_{(1,2,1)}(q)$ with seam $(r, a, \kappa) = (1, 2, 1)$. The q -series at the isotropic conformal point with real q is

$$\begin{aligned} Z_{(1,2,1)}(q) &= \hat{\chi}_{1,2}(\hat{\chi}_{1,1} + 2\hat{\chi}_{1,3}) + \hat{\chi}_{3,2}(\hat{\chi}_{3,1} + 2\hat{\chi}_{3,3}) \\ &= (\chi_{1,2} + \chi_{1,4})(\chi_{1,1} + \chi_{1,5} + 2\chi_{1,3}) + (\chi_{3,2} + \chi_{3,4})(\chi_{3,1} + \chi_{3,5} + 2\chi_{3,3}) \\ &= q^{-1/15}(2q^{11/120} + q^{1/8} + q^{17/40} + 2q^{71/120} + 2q^{19/24} + q^{37/40} + 4q^{131/120} + o(q^{131/120})) \end{aligned} \quad (5.23)$$

so that the exponents, counting degeneracies, are given by the sequence

$$\{x_n\} = \{\frac{11}{120}, \frac{11}{120}, \frac{1}{8}, \frac{17}{40}, \frac{71}{120}, \frac{71}{120}, \frac{19}{24}, \frac{19}{24}, \frac{37}{40}, \frac{131}{120}, \frac{131}{120}, \dots\} \quad (5.24)$$

A plot of our numerical data is shown in Fig. 6. Notice that some eigenvalues cross so that it is not possible to simply order the eigenvalues according to their magnitudes at a given value of N and this complicates the extrapolation procedure. Although we have not systematically done so, it is possible to remove this ambiguity in the identification of each eigenvalue at a given N by examining the patterns of the zeros of the eigenvalue $T_n^{(N)}(u)$ in the complex u -plane as explained in [29]. The theoretical data (5.24) is to be compared with our numerical values of $\{x_n\}$ for the $(1, 2, 1)$ seam shown in Table 7. The agreement over the first 10 levels is certainly good enough to unequivocally identify the $(1, 2, 1)$ integrable seam as giving rise to the $(1, 2, 1)$ twisted partition function.

Typical numerical data for two other seams is also shown in Table 7. In this way we can identify all of the integrable seams with the corresponding twisted boundary conditions in Table 6 given by Petkova and Zuber [7]. In particular, we confirm that our integrable seams give a realization of the complete set of conformal twisted boundary conditions for the 3-state Potts model.

(1, 2, 1)										
n	0	1	2	3	4	5	6	7	8	9
Exact	$\frac{11}{120}$	$\frac{11}{120}$	$\frac{1}{8}$	$\frac{17}{40}$	$\frac{71}{120}$	$\frac{71}{120}$	$\frac{19}{24}$	$\frac{19}{24}$	$\frac{37}{40}$	$\frac{131}{120}$
Num.	0.0915	0.0915	0.1250	0.4258	0.5934	0.5934	0.7969	0.7969	0.9215	1.0421
diff.	10^{-4}	10^{-4}	$3 \cdot 10^{-5}$	$8 \cdot 10^{-4}$	0.0018	0.0018	0.0053	0.0053	0.0035	0.0496
(1, 3, 1)										
Exact	$\frac{2}{15}$	$\frac{7}{15}$	$\frac{7}{15}$	$\frac{2}{3}$	$\frac{2}{3}$	$\frac{17}{15}$	$\frac{17}{15}$	$\frac{4}{3}$	$\frac{22}{15}$	$\frac{22}{15}$
Num.	0.1335	0.4658	0.4658	0.6681	0.6681	1.1640	1.1640	1.3364	1.4445	1.4445
diff.	10^{-4}	$8 \cdot 10^{-4}$	$8 \cdot 10^{-4}$	0.0014	0.0014	0.0306	0.0306	0.0030	0.0222	0.0222
(3, 1, 2)										
Exact	$\frac{1}{20}$	$\frac{3}{20}$	$\frac{3}{20}$	$\frac{11}{20}$	$\frac{11}{20}$	$\frac{13}{20}$	$\frac{13}{20}$	$\frac{21}{20}$	$\frac{21}{20}$	$\frac{21}{20}$
Num.	0.0492	0.1501	0.1501	0.5479	0.5479	0.6503	0.6503	1.0577	1.0577	1.0629
diff.	$8 \cdot 10^{-4}$	10^{-4}	10^{-4}	0.0021	0.0021	$3 \cdot 10^{-4}$	$3 \cdot 10^{-4}$	0.0077	0.0077	0.0129

Table 7: Numerical exponents x_n for the (A_4, D_4) minimal model with seams of type $(r, a, \kappa) = (1, 2, 1), (1, 3, 1)$ and $(3, 1, 2)$.

5.5 Numerical spectra of (A_6, D_5)

The numerical spectra of the minimal (A_6, D_5) model can be obtained similarly to the (A_4, D_4) model. The graph D_5 , however, is a Type II graph with parent graph A_7 . The integrable seams are thus labelled by $(r, s) \in (A_6, A_7)$ where the s -type fusion seams are subject to the fused adjacency matrices n_s of D_5 . Let $\eta = \sigma$ implement the \mathbf{Z}_2 transposition (4 5) interchanging nodes 4 and 5. We observe that the spectra are the same for the seams $(r, 2, 1)$ and $(r, 2, 2)$. Similarly, the spectra are the same for the seams $(r, s, 1)$ and $(r, 8-s, 2)$ for all $1 \leq s \leq 7$. This is in accord with the fused adjacency matrix relations

$$n_7 = \sigma, \quad n_2 = n_6, \quad n_i = n_{8-i} \quad n_7 = n_7 n_{8-i}, \quad 1 \leq i \leq 7 \quad (5.25)$$

Our data for seams of type $(r, a, \kappa) = (1, 2, 1)$, $(3, 3, 1)$ and $(1, 1, 2)$ are shown in Table 8.

(1, 2, 1)										
n	0	1	2	3	4	5	6	7	8	9
Exact	$\frac{23}{224}$	$\frac{23}{224}$	$\frac{27}{224}$	$\frac{5}{32}$	$\frac{83}{224}$	$\frac{107}{224}$	$\frac{135}{224}$	$\frac{135}{224}$	$\frac{167}{224}$	$\frac{167}{224}$
Num.	0.102	0.102	0.1201	0.1562	0.3728	0.481	0.6074	0.6074	0.7527	0.7527
$ diff. $	$7 \cdot 10^{-4}$	$7 \cdot 10^{-4}$	$5 \cdot 10^{-4}$	$5 \cdot 10^{-5}$	0.0023	0.0033	0.0047	0.0047	0.0071	0.00714
(3, 3, 1)										
n	$\frac{1}{28}$	$\frac{1}{28}$	$\frac{1}{14}$	$\frac{9}{112}$	$\frac{9}{112}$	$\frac{15}{112}$	$\frac{1}{7}$	$\frac{1}{7}$	$\frac{3}{14}$	$\frac{25}{112}$
Exact	$\frac{1}{28}$	$\frac{1}{28}$	$\frac{1}{14}$	$\frac{9}{112}$	$\frac{9}{112}$	$\frac{15}{112}$	$\frac{1}{7}$	$\frac{1}{7}$	$\frac{3}{14}$	$\frac{25}{112}$
Num.	0.036	0.036	0.0722	0.0813	0.0813	0.1354	0.1459	0.1459	0.215	0.2275
$ diff. $	$2 \cdot 10^{-4}$	$2 \cdot 10^{-4}$	$7 \cdot 10^{-4}$	$9 \cdot 10^{-4}$	$9 \cdot 10^{-4}$	0.0015	0.0031	0.0031	0.0007	0.0043
(1, 1, 2)										
n	$\frac{3}{112}$	$\frac{15}{112}$	$\frac{5}{16}$	$\frac{4}{7}$	$\frac{4}{7}$	$\frac{99}{112}$	$\frac{115}{112}$	$\frac{115}{112}$	$\frac{127}{112}$	$\frac{127}{112}$
Exact	$\frac{3}{112}$	$\frac{15}{112}$	$\frac{5}{16}$	$\frac{4}{7}$	$\frac{4}{7}$	$\frac{99}{112}$	$\frac{115}{112}$	$\frac{115}{112}$	$\frac{127}{112}$	$\frac{127}{112}$
Num.	0.027	0.1347	0.3126	0.569	0.569	0.8785	1.0310	1.0310	1.1673	1.1673
$ diff. $	$2 \cdot 10^{-4}$	$8 \cdot 10^{-4}$	$1 \cdot 10^{-4}$	0.0026	0.0026	0.0054	0.0042	0.0042	0.033	0.033

Table 8: Numerical exponents x_n of the (A_6, D_5) minimal model with seams of type $(r, a, \kappa) = (1, 2, 1)$, $(3, 3, 1)$ and $(1, 1, 2)$.

(1, 5, 1)										
n	0	1	2	3	4	5	6	7	8	9
Exact	$\frac{2}{45}$	$\frac{2}{15}$	$\frac{4}{15}$	$\frac{8}{15}$	$\frac{8}{15}$	$\frac{29}{45}$	$\frac{29}{45}$	$\frac{14}{15}$	$\frac{47}{45}$	$\frac{47}{45}$
Num.	0.0447	0.1345	0.2688	0.5267	0.5267	0.6438	0.6438	0.9625	1.0256	1.0256
$ diff. $	$2 \cdot 10^{-4}$	0.0011	0.0021	0.0066	0.0066	$7 \cdot 10^{-4}$	$7 \cdot 10^{-4}$	0.0292	0.0188	0.0188
(8, 2, 1)										
n	$\frac{13}{120}$	$\frac{13}{120}$	$\frac{43}{360}$	$\frac{17}{120}$	$\frac{7}{40}$	$\frac{41}{120}$	$\frac{151}{360}$	$\frac{61}{120}$	$\frac{73}{120}$	$\frac{73}{120}$
Exact	$\frac{13}{120}$	$\frac{13}{120}$	$\frac{43}{360}$	$\frac{17}{120}$	$\frac{7}{40}$	$\frac{41}{120}$	$\frac{151}{360}$	$\frac{61}{120}$	$\frac{73}{120}$	$\frac{73}{120}$
Num.	0.1081	0.1081	0.1193	0.1408	0.1749	0.3461	0.4214	0.5061	0.6252	0.6252
$ diff. $	$2 \cdot 10^{-4}$	$2 \cdot 10^{-4}$	$1 \cdot 10^{-4}$	$8 \cdot 10^{-4}$	$8 \cdot 10^{-4}$	0.0044	0.0019	0.0022	0.0169	0.0169
(3, 5, 2)										
n	$\frac{1}{20}$	$\frac{1}{20}$	$\frac{1}{12}$	$\frac{5}{36}$	$\frac{5}{36}$	$\frac{7}{36}$	$\frac{49}{180}$	$\frac{49}{180}$	$\frac{79}{180}$	$\frac{79}{180}$
Exact	$\frac{1}{20}$	$\frac{1}{20}$	$\frac{1}{12}$	$\frac{5}{36}$	$\frac{5}{36}$	$\frac{7}{36}$	$\frac{49}{180}$	$\frac{49}{180}$	$\frac{79}{180}$	$\frac{79}{180}$
Num.	0.0503	0.0503	0.0854	0.1433	0.1433	0.1941	0.2741	0.2741	0.4276	0.4276
$ diff. $	$3 \cdot 10^{-4}$	$3 \cdot 10^{-4}$	0.0020	0.0044	0.0044	0.0004	0.0018	0.0018	-0.0112	0.0112

Table 9: Numerical exponents x_n of the (A_8, D_6) minimal model with seams of type $(r, a, \kappa) = (1, 5, 1)$, $(8, 2, 1)$ and $(3, 5, 2)$.

5.6 Numerical spectra of (A_8, D_6)

For D_6 we have fewer data points than for D_4 so the precision of the extrapolated values of the exponents is not as good. Nevertheless, the characteristic degeneracies of the exponents in the twisted partition functions are faithfully reproduced. Our data for seams of type $(r, a, \kappa) = (1, 5, 1)$, $(8, 2, 1)$ and $(3, 5, 2)$ are shown in Table 9.

As dictated by symmetry we observe generally, for $(A_{4\ell-4}, D_{2\ell})$, that the a -type seams $(1, 2\ell-1, 1)$ and $(1, 2\ell, 1)$ give the same spectra for the transfer matrices. This is in accord with the symmetry of the graph fusion matrices. Indeed, if σ implements the \mathbf{Z}_2 transposition for $(A_{4\ell-4}, D_{2\ell})$ then

$$\sigma \hat{N}_{2\ell-1} = \hat{N}_{2\ell} \sigma \quad (5.26)$$

so that $\hat{N}_{2\ell-1}$ is similar to $\hat{N}_{2\ell}$ under interchange of the nodes $2\ell-1$ and 2ℓ .

6 Discussion

In this paper we have constructed integrable seams for each twisted conformal boundary condition $x = (r, a, b, \kappa)$ of the A - D - E $sl(2)$ minimal models. Our construction labels are identical to the conformal labels of Petkova and Zuber. For E_7 , we have not succeeded in constructing single integrable seams for the special seams denoted (r, X) , even though we have constructed integrable seams of type $(r, 6, 2, 1)$ and $(r, 4, 2, 1)$ which suffice to give the partition functions, so these seams remain somewhat mysterious.

The construction of our integrable seams involves a new type of fusion, related to the graph fusion matrices \hat{N}_a and labelled by the nodes a of the graph G , rather than the usual Young tableaux. We find that the left-and right-chiral halves of the Ocneanu fusion algebra are related to the braid limits $u \rightarrow \pm i\infty$ of the seam weights. The quantum symmetries and twisted conformal partition functions have been verified numerically for the A_L , $L = 3, 4, 5, 6, 7, 8, 9$ and D_L , $L = 4, 5, 6$ cases. In general, the numerics reproduce the first 10 exponents to about a 1 or 2% accuracy. Together with the agreement of the exact degeneracies, the numerics give strong evidence of the identification of our seams with the corresponding twisted conformal boundary conditions. The origin of non-commutativity in the Ocneanu graph fusion algebra is traced to the existence of graph automorphisms which do not commute with the fusions.

Lastly, we point out that the parameter ξ appearing in the integrable seams is an arbitrary complex parameter. We have fixed its value to ensure conformal boundary conditions in the continuum scaling limit. By choosing it to have an imaginary part that scales appropriately with N (the number of columns in the transfer matrix), it is possible [30] to perturb the boundary away from the conformal fixed point. This will induce renormalization group flows between the fixed points representing the various twisted conformal boundary conditions.

Acknowledgements

This research is supported by the Australian Research Council. Part of this work was done while CHOC and PAP were visiting IPAM, UCLA. We thank Valya Petkova and Jean-Bernard Zuber for their continued interest in this work and for comments on the manuscript.

References

- [1] Roger E. Behrend, Paul A. Pearce, and Jean-Bernard Zuber. Integrable boundaries, conformal boundary conditions and A - D - E fusion rules. *J. Phys. A*, 31(50):L763–L770, 1998. ISSN 0305-4470. [hep-th/9807142](#).
- [2] Roger E. Behrend, Paul A. Pearce, Valentina B. Petkova, and Jean-Bernard Zuber. On the classification of bulk and boundary conformal field theories. *Phys. Lett. B*, 444(1-2):163–166, 1998. ISSN 0370-2693. [hep-th/9809097](#).
- [3] Roger E. Behrend, Paul A. Pearce, Valentina B. Petkova, and Jean-Bernard Zuber. Boundary conditions in rational conformal field theories. *Nuclear Phys. B*, 579(3):707–773, 2000. ISSN 0550-3213. [hep-th/9908036](#).
- [4] Roger E. Behrend and Paul A. Pearce. Integrable and conformal boundary conditions for $\widehat{\text{sl}}(2)$ A - D - E lattice models and unitary minimal conformal field theories. In *J. Stat. Phys.*, 102:577–640, 2001. [hep-th/0006094](#).
- [5] V.B. Petkova and J.-B. Zuber. BCFT: from the boundary to the bulk. Nonperturbative Quantum Effects 2000. [hep-th/0009219](#).
- [6] Robert Coquereaux. Notes on the quantum tetrahedra. *Moscow Math. J.*, 2:41–80, 2002. [math-ph/0011006](#).
- [7] V. B. Petkova and J.-B. Zuber. Generalised twisted partition functions. *Phys. Lett. B*, 504(1-2):157–164, 2001. ISSN 0370-2693. [hep-th/0011021](#).
- [8] V.B. Petkova and J.-B. Zuber. The many faces of Ocneanu cells. *Nuclear Phys. B*, 603:449–496, 2001. ISSN 0550-3213. [hep-th/0101151](#).
- [9] A. Cappelli, C. Itzykson, and J. B. Zuber. The A - D - E classification of minimal and $A_1^{(1)}$ conformal invariant theories. *Comm. Math. Phys.*, 113(1):1–26, 1987. ISSN 0010-3616.
- [10] Christian Mercat and Paul A. Pearce. Integrable and Conformal Boundary Conditions for \mathbf{Z}_k Parafermions on a Cylinder. *J. Phys. A*, 34(3):5751–5771, 2001. ISSN 0305-4470. [hep-th/0103232](#).
- [11] Vincent Pasquier. Two-dimensional critical systems labelled by Dynkin diagrams. *Nuclear Phys. B*, 285(1):162–172, 1987. ISSN 0550-3213.
- [12] Christoph Richard and Paul A. Pearce. Integrable lattice realizations of $N = 1$ superconformal boundary conditions. *Nucl. Phys. B*, 631:447–470, 2002. [hep-th/0109083](#).
- [13] C. H. Otto Chui, Christian Mercat, William P. Orrick, and Paul A. Pearce. Integrable lattice realizations of conformal twisted boundary conditions. *Phys. Lett. B*, 517:429–435, 2001.

[14] Adrian Ocneanu. Paths on Coxeter Diagrams: From Platonic Solids and Singularities to Minimal Models and Subfactors. *Lectures on Operator Theory, Fields Institute, AMS*, 1995.

[15] Adrian Ocneanu. The classification of subgroups of quantum $SU(N)$. Bariloche, 2000. <http://www.cpt.univ-mrs.fr/~coque/Bariloche2000/Bariloche2000.html>

[16] Robert Coquereaux and Gil Schieber. Twisted partition functions for $A D E$ boundary conformal field theories and Ocneanu algebras of quantum symmetries. *J. Geom. Phys.*, 42:216–258, 2002. [hep-th/0107001](#).

[17] Rodney J. Baxter. *Exactly solved models in statistical mechanics*. Academic Press Inc. [Harcourt Brace Jovanovich Publishers], London, 1989. ISBN 0-12-083182-1. Reprint of the 1982 original.

[18] George Andrews, Rodney J. Baxter and Peter J. Forrester. Eight-vertex SOS Model and generalized Rogers-Ramnujan-type identities. *J. Stat. Phys.*, 35:193–266, 1984.

[19] Uwe Grimm. Spectrum of a duality-twisted Ising quantum chain. *J. Phys. A*, 35:L25–L30, 2002.

[20] Uwe Grimm. Duality and conformal twisted boundaries in the Ising model. [hep-th/0209048](#), 2002.

[21] J.-B. Zuber. Discrete symmetries of conformal theories. *Phys. Lett. B*, 176:127–129, 1986.

[22] S. Lienart, P. Ruelle and O. Verhoeven. On discrete symmetries in $su(2)$ and $su(3)$ affine theories and related graphs. *Nucl.Phys. B*, 592:479–511, (2001).

[23] Je-Young Choi, Doochul Kim, and Paul A. Pearce. Boundary conditions and inversion identities for solvable lattice models with a sublattice symmetry. *J. Phys. A*, 22(10):1661–1671, 1989. ISSN 0305-4470.

[24] Roger E. Behrend, Paul A. Pearce, and David L. O’Brien. Interaction-round-a-face models with fixed boundary conditions: the ABF fusion hierarchy. *J. Stat. Phys.*, 84(1-2):1–48, 1996. ISSN 0022-4715. [hep-th/9507118](#).

[25] Valentina Petkova and Jean-Beranrd Zuber. Conformal Field Theories, Graphs and Quantum Algebras. *Progress in Math.*, in MathPhys Odyssey 2001 –Integrable Models and Beyond, ed. M. Kashiwara and T. Miwa, 2001. Birkhauser 415–435, 2002.

[26] C. H. Otto Chui, Christian Mercat, and Paul A. Pearce. Integrable boundaries and universal TBA functional equations. *Progress in Math.*, in MathPhys Odyssey 2001 –Integrable Models and Beyond, ed. M. Kashiwara and T. Miwa, 2001. Birkhauser 391–413, 2002.

- [27] Stephen Wolfram. The Mathematica Book, 4th ed. Wolfram Media/Cambridge University Press, 1999.
- [28] J. M. van den Broeck and L. W. Schwartz. *Siam J. Math. Anal.*, 10:639, 1979.
- [29] Andreas Klümper and Paul A. Pearce. Analytic calculation of scaling dimensions: tricritical hard squares and critical hard hexagons. *J. Stat. Phys.*, 64:13–76, 1991.
- [30] Giovanni Feverati, Paul A. Pearce and Francesco Ravanini. Lattice approach to excited TBA boundary flows: tricritical Ising model. *Phys. Lett. B*, 534:216–223, 2002.